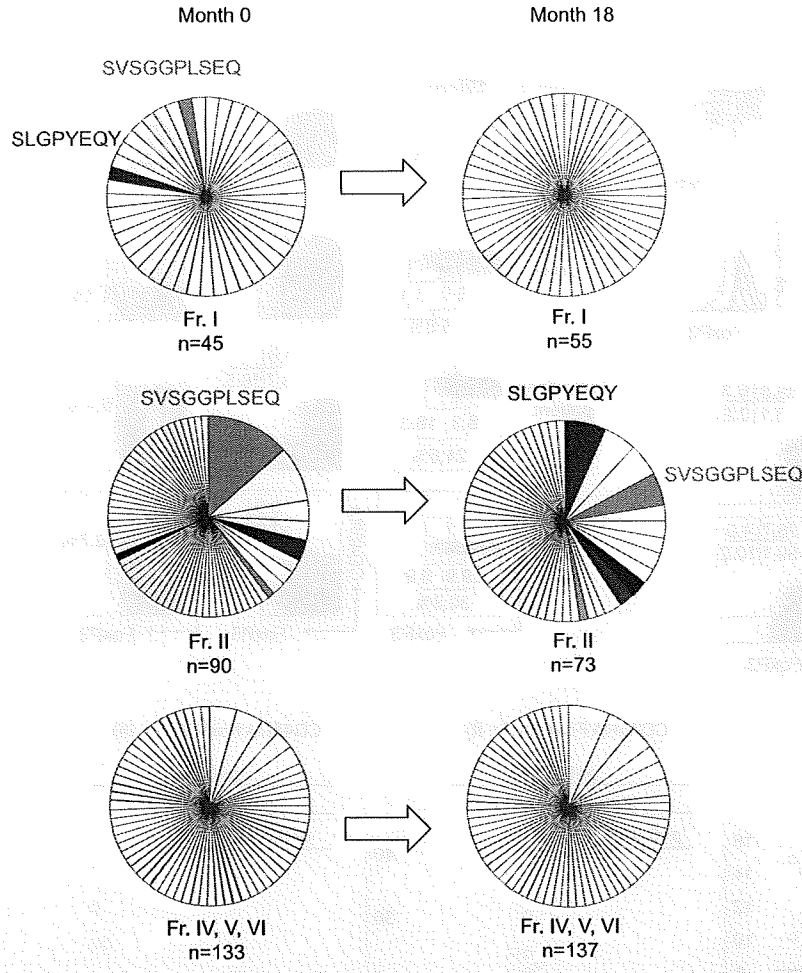


**Figure 5. Longitudinal TCR Repertoire Analysis in FoxP3+ Cell Subpopulations**

TCRBV5+CD4+ T cells belonging to indicated Treg or non-Treg cell fractions were FACS sorted as a single cell at indicated time points into wells of PCR plates. By RT-PCR and TCR sequencing, the frequencies of individual sequences were assessed. Empty slices correspond to sequences that were found only once in only one subset. Persistent clones are color highlighted. Slice size is proportional to the number of occurrences of the corresponding TCR sequences. The total number of sequences successfully analyzed in each subset is indicated.

controls signaling thresholds in lymphocytes, hence their state of differentiation and activation (Hermiston et al., 2003). The three subpopulations are CD45RA$^-$FoxP3$^{hi}$CD4$^+$ activated Treg cells and CD45RA$^+$FoxP3$^{lo}$CD4$^+$ resting Treg cells, both of which are potently suppressive in vitro, and cytokine-secreting nonsuppressive CD45RA$^-$FoxP3$^{lo}$CD4$^+$ non-Treg cells.

The distinction of FoxP3$^+$ subpopulations revealed the differentiation pathways of Treg cell subpopulations. First, most of FoxP3$^{hi}$ aTreg cells originate from rTreg cells as shown in vitro and in vivo, although some FoxP3$^{hi}$ Treg cells may arise from FoxP3$^-$CD4$^+$ non-Treg cells (Vukmanovic-Stejic et al., 2006). Second, a large proportion of FoxP3$^{hi}$ aTreg cells is highly proliferative in vivo and appears to be recently activated, although most rTreg cells are in a resting state. Once rTreg cells are stimulated, they upregulate FoxP3 expression, differentiate to aTreg cells, and proliferate. In addition to these results obtained by direct ex vivo analysis of the subpopulations and by their transfer to NOG mice, our longitudinal study of the repertoire of a particular TCR Vβ subfamily in a single individual provides further evidence that the conversion of rTreg to aTreg cells physiologically occurs in vivo. In our current analysis, dominant clones found in the rTreg cell population were found 18 months later in the aTreg, but not rTreg, cell population. This indicates that the clones have preferentially expanded after differentiating to aTreg cells, as suggested by the high rate of Ki-67$^+$ cells in the aTreg cell population. The presence of such dominant T cell clones over a long period of time is a key feature of the aTreg cell population (C.P. and G.G., unpublished data). This also indicates that the TCR repertoire of Treg cells adaptively changes with clonal expansion especially in aTreg cells. Considering that aTreg cells rapidly die in vitro and that the immune system is constantly challenged by exogenous and endogenous antigens, it is highly likely that the maintenance of the pool of aTreg cells is the consequence of a tight balance between the constant development of aTreg cells from activated and proliferating rTreg cells and their death after exerting suppression. Further, aTreg cells control rTreg cell expansion in a feedback manner, contributing to the maintenance of the balance. FoxP3$^{hi}$ aTreg cells thus appear to be terminally differentiated Treg cells; yet it remains to be determined whether the aTreg cell population contains a memory type long-living Treg cells. Given that aTreg cells die rapidly and that rTreg cells are highly proliferative upon stimulation, attempts to expand Treg cells ex vivo for cell therapy should be focused on rTreg cells as proposed by others (Hoffmann et al., 2006). It needs to be determined whether rTreg cells are constantly produced by the thymus, or whether they have a high renewal capacity in the periphery, or both.

Our study has clearly shown that human FoxP3$^+$CD4$^+$ T cells contain cytokine-secreting nonsuppressive effector T cells that display low expression of FoxP3. These nonsuppressive FoxP3$^{lo}$CD45RA$^-$CD4$^+$ T cells (Fr. III) may correspond to recently described activation-induced FoxP3-expressing cells that transiently express FoxP3 in vitro (Allan et al., 2007; Gavin et al., 2006; Tran et al., 2007; Wang et al., 2007). Supporting this notion, although the 5′ flanking region of the *FOXP3* gene in FoxP3$^{lo}$CD45RA$^-$CD4$^+$ T cells is highly demethylated, the STAT5-responsive region is poorly demethylated, suggesting that they may be unstable in maintaining FoxP3 expression through

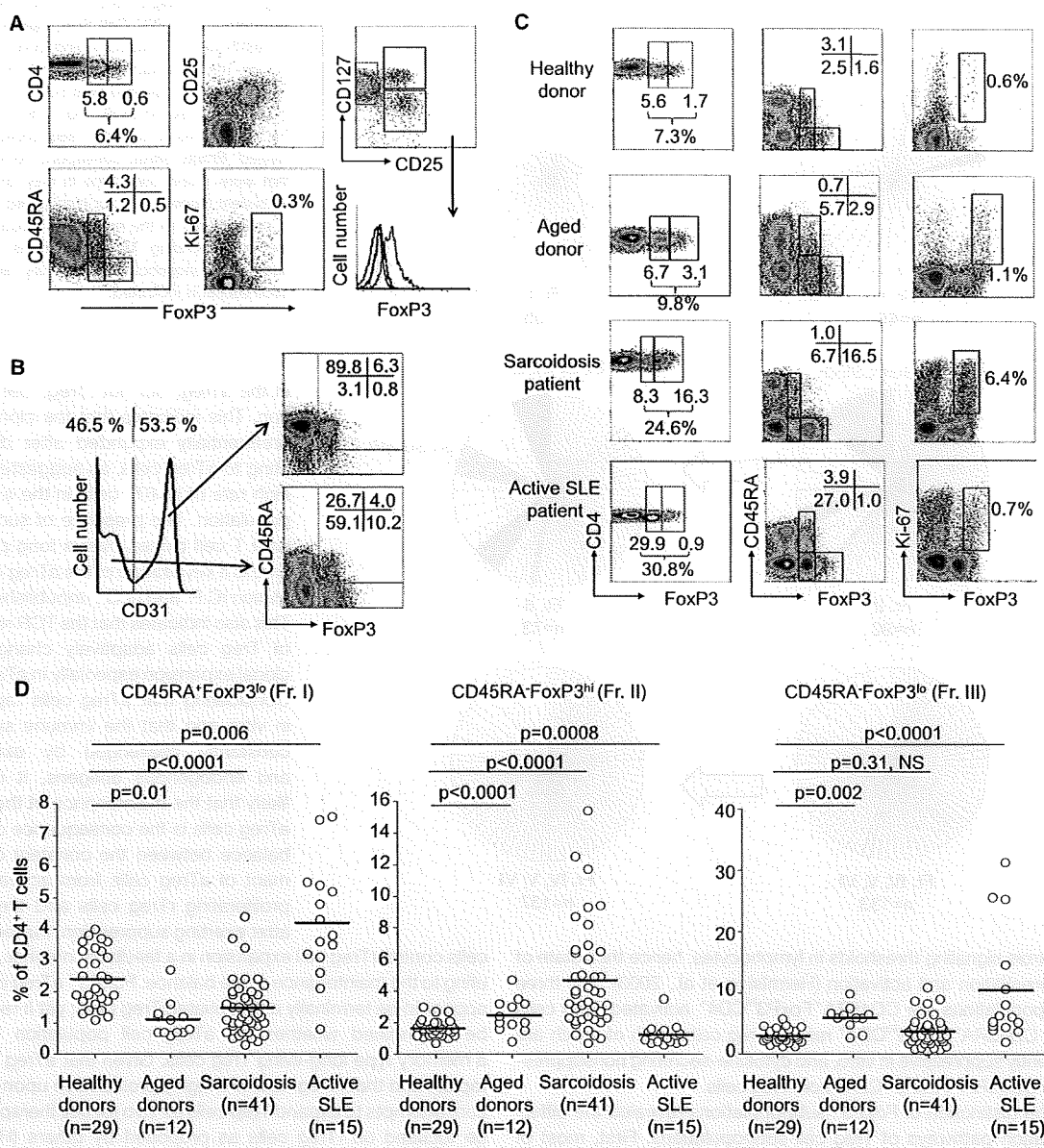


**Figure 6. Variations in FoxP3+ Cell Subpopulations under Physiological and Disease Conditions**

(A) Flow cytometry of PBMCs gated on $CD4^+$ T cells isolated from cord blood. A representative of four samples.

(B) Expression of CD45RA and FoxP3 by gated $CD31^+$ or $CD31^-$ $CD4^+$ T cells. Numbers indicate percentage in each quadrant. A representative of four independent experiments.

(C) Flow cytometry of PBMCs gated on $CD4^+$ T cells isolated from a 29-year-old healthy adult, an 88-year-old donor, and two patients with active sarcoidosis or active SLE. Percentage of each quadrant in each staining combination is shown.

(D) Percentages of each $FoxP3^+$ subset among $CD4^+$ T cells in indicated numbers of patients with active sarcoidosis, active SLE, aged donors (between 79 and 90 years old), and healthy donors (between 18 and 40 years old). Red horizontal bars represent mean percentage. Statistical comparisons were performed by nonparametric Mann-Whitney U test. NS, not significant.

STAT5 signaling. The notion is also supported by recent reports showing that activation-induced $FoxP3^+CD4^+$ T cells have *FOXP3* DNA significantly less demethylated than bona fide Treg cells (Baron et al., 2007; Janson et al., 2008). In addition, although CD127 is a convenient marker for isolating $FoxP3^+$ cells as $CD25^{hi}CD127^{lo}CD4^+$ T cells (Liu et al., 2006; Seddiki et al., 2006), it is of note that they also include $FoxP3^+$ non-Treg cells. We therefore propose that the combination of CD25 and CD45RA is so far the best markers for purifying human $FoxP3^+$ Treg cells as rTreg and aTreg cells.

We noticed in microarray analysis that RORC, the human ortholog of murine RORγt, a major transcription factor for Th17 cell differentiation (Ivanov et al., 2006), was highly upregulated in both Fr. II and III and much less in Fr. I. Indeed, FoxP3$^{lo}$ memory-like non-Tregs (Fr. III) were the highest producers of IL-17 among CD4$^+$ T cells. These results support recent findings in mice that FoxP3-RORγt double-positive CD4$^+$ T cells can convert into either Treg cells or Th17 cells (Yang et al., 2008a; Zhou et al., 2008). AHR was recently shown in mice to be critical for the differentiation of naive T cells to Th17 versus FoxP3$^+$ Treg cells (Quintana et al., 2008; Veldhoen et al., 2008). Our finding of upregulated AHR repressor in aTreg cells therefore suggests that differentiation of FoxP3$^-$CD4$^+$ T cells to aTreg cells might be regulated through the modulation of AHR activity by AHR repressor. Further study is required to determine how the expression amount of FoxP3 in each FoxP3$^+$ subpopulation contributes to the function of each subset (e.g., suppression and IL-17 production) through interaction with other molecules including RORC.

This study has revealed several key features of Treg cell-mediated suppression in vitro. First, challenging the commonly accepted notion that Treg cells are anergic in vitro, human Treg cells proliferate and die, although the degree of their proliferation is much lower than that of non-Treg cells when Treg cells and non-Treg cells are separately stimulated and compared. Further, the hypoproliferation observed with CD25$^{hi}$CD4$^+$ T cells can be attributed, in part, to the suppression of rTreg cell proliferation by aTreg cells and also to the death of the latter. These findings mean that thymidine uptake by whole cocultured cells in Treg cell assay may not be accurate to monitor responder cell proliferation in the presence of Treg cells. Second, CTLA-4 expression in aTreg cells, but not in rTreg cells, suggests that aTreg cells are the main effectors of suppression as shown by the fact that Treg cell-specific deficiency impairs Treg cell suppressive function in vivo and in vitro in mice (Wing et al., 2008). Further, FoxP3$^+$ Treg cells out-compete naive T cells in in vitro aggregation around dendritic cells and downregulate their expression of CD80 and CD86 in a CTLA-4-dependent fashion (Onishi et al., 2008). It is likely in humans that, upon activation, rTreg cells differentiate to aTreg cells and exert suppression in vitro through these mechanisms. As another possibility, rTreg and aTreg cells might use different suppressive mechanisms by secreting different immunosuppressive cytokines such as IL-10 and TGF-β (Ito et al., 2008). Our microarray analysis indeed indicates that aTreg cells are more active in IL-10 transcription but less active in TGF-β transcription than rTreg cells. Further study is required to determine whether Treg cells use multiple suppressive mechanisms depending on their differentiation status (Sakaguchi et al., 2008).

Finally, supporting physiological and clinical relevance of distinguishing subpopulations of FoxP3$^+$ T cells, rTreg and aTreg cells can be clearly identified with different proportions in cord blood of healthy newborns, PBL of aged individuals, and patients with SLE or sarcoidosis. In cord blood, we unexpectedly found a small but always detectable population of CD45RA$^{lo}$Ki-67$^+$FoxP3$^{hi}$CD4$^+$ T cells that corresponded to adult aTreg cells. This finding suggests that even in fetuses, natural rTreg cells are constantly activated by endogenous self antigens and exogenous antigens derived from maternal circulation. An opposite trend exists in aged donors, who had high proportions of aTreg cells and low but still detectable proportions of rTreg cells. Because of thymus involution observed in aged individuals, one can speculate that, like conventional naive CD4$^+$ T cells (Vrisekoop et al., 2008), rTreg cells can be generated in the periphery in aged individuals to compensate for decreased thymic production of Treg cells; alternatively, but not exclusively, aTreg cells may homeostatically expand to counterbalance the lack of rTreg cells in the periphery. Under pathological conditions, a high prevalence of aTreg cells and a decrease in the rTreg cell population in sarcoidosis suggests that rTreg cells may be swiftly converted into aTreg cells immediately after having emigrated from the thymus or having been peripherally generated. In contrast, in active SLE, the number of aTreg cells decreased while that of rTreg cells remained normal or increased, with a notable increase in FoxP3$^{lo}$CD4$^+$ non-Treg cells. This also confirms the FoxP3$^{lo}$CD45RA$^-$ memory/effector-like non-Treg cell subset as a discrete population among FoxP3$^+$ CD4$^+$ T cells. Further functional analysis is required to interpret these anomalies and variations in disease states (Taflin et al., 2009). Yet, analysis of Treg cell function by dissecting FoxP3$^+$ cells into three subpopulations is instrumental for understanding pathophysiology of immunological diseases.

In conclusion, we propose a definition of human FoxP3$^+$ Treg cell subsets based on in vitro and in vivo features of FoxP3-expressing CD4$^+$ T cells. Functional and numerical analysis of each subset will help to understand and control immune responses in normal and disease states.

## EXPERIMENTAL PROCEDURES

### Human Samples

Blood samples were obtained from young healthy adult volunteers (18–40 years old), from aged control donors (79–90 years old), and from active sarcoidosis or active SLE patients and cord blood samples from full-term neonates who had no hereditary disorders, hematologic abnormalities, or infectious complications. Aged donors had no acute or chronic inflammatory or infectious disease, ongoing thrombosis, or neoplasia. Diagnosis of active SLE and sarcoidosis were made according to previously described criteria (Miyara et al., 2005, 2006). All patients were newly diagnosed and not medicated with steroid or immunosuppressant. The study was done according to the Helsinki declaration with the approval from the human ethics committee of the Institute for Frontier Medical Sciences, Kyoto University and from Comité Consultatif de Protection des Personnes dans la Recherche Biomédicale of Pitié-Salpétrière Hospital, Paris. Human peripheral blood PBMC were prepared by Ficoll gradient centrifugation. Lymphocyte subpopulations was isolated by a MoFLo cell sorter (Dako) after positive magnetic cell separation of CD4$^+$ T cells by CD4$^+$ T cell MACS beads (Miltenyi Biotec). Purity of isolated cells was always >95% (Figure S1). Autologous CD14$^+$ and CD19$^+$ cells positively selected by mixed MACS and irradiated (50 Gy) were used as accessory cells.

### Mice

NOG mice described previously (Hiramatsu et al., 2003) were injected intravenously with 3.5–5 × 10$^7$ human PBMCs. The mice were maintained in our animal facility and treated in accordance with the guidelines of Kyoto University.

### Flow Cytometry

Freshly obtained or in vitro cultured lymphocytes and human lymphocytes isolated from NOG mouse spleens were stained with anti-hCD4 (-PerCP-Cy5.5 from BD biosciences or -APC from R&D Systems), anti-hCD25 (-PE or -PE-Cy5 from BD), anti-hCD45RO (-PE from Beckman Coulter and PE-Cy7 from

BD), anti-hCD45RA (-PE-Cy7 from BD or -FITC from Beckman Coulter), anti-ICOS (-FITC from e-Bioscience), anti-HLA-DR (-PE from BD biosciences), anti-CD31 (-APC from e-Bioscience), anti-hCD127 (-PE from Beckman Coulter and -PE-Cy5 from e-bioscience), and 7-AAD (Dako). Intracellular detection of FoxP3 with anti-hFoxP3 (PE or Alexa Fluor 647, clone 236A/E7 [e-Bioscience] or clone 259D [BD biosciences]) and of Ki-67 antigen with Ki-67 antibody (FITC or PE from BD) was performed on fixed and permeabilized cells via Cytofix/Cytoperm (e-Bioscience). For detection of intracellular cytokine production, $CD4^+$ T cells were stimulated with 20 ng/ml PMA and 1 μM ionomycin in the presence of Golgi-Stop (BD Biosciences) for 5 hr and then stained with anti-hFoxP3-PE, Ki-67-FITC, anti-IL2-APC (BD Biosciences), anti-IFN-γ-APC (BD), or anti-IL-17-Alexa Fluor 647 (e-Bioscience) after fixation and permeabilization. Data acquired by FACSCalibur (Becton Dickinson) were analyzed with WinMDI 2.9 software (http://facs.scripps.edu/software.html). Statistical comparisons were performed with the nonparametric Mann-Whitney U test.

### Cell Culture and Suppression Assay

RPMI 1640 medium supplemented with 10% fetal bovine serum, 100 IU/ml penicillin, and 100 μg/ml streptomycin (Sigma, St. Louis, MO) was used for T cell culture. Cells were labeled with 1 μM CFSE (Dojindo and Invitrogen). In suppression assays, unless otherwise indicated, $1 \times 10^4$ CFSE-labeled responder $CD25^-CD45RA^+CD4^+$ T cells were cocultured with $1 \times 10^4$ unlabeled cells assessed for their suppressive capacity and $1 \times 10^5$ irradiated autologous accessory cells and were stimulated with 0.5 μg/mL plate-bound anti-CD3 (OKT3 mAb) in 96-well round-bottom plate in supplemented RPMI medium. Proliferation of CFSE-labeled cells was assessed by flow cytometry after 84–90 hr of culture. Percent suppression was calculated by dividing the number of proliferating CFSE-diluting responder cells in the presence of suppressor cells at a 1 to 1 ratio by the number of proliferating responder cells when cultured alone, and multiplied by 100.

### *FOXP3* Gene DNA Methylation

The genomic DNA from purified human $CD4^+$ T cell subsets was extracted by the Blood & Tissue Genomic DNA Extraction System (Viogene). Genomic DNA from purified cells was bisulfite converted by the EpiTect Bisulfite Kit (QIAGEN) according to the manufacturer's instructions. DNA was then subjected to PCR with primers for amplification of specific targets in bisulfite-treated DNA. The PCR products obtained were cloned into the pGEM-T Easy vector (Promega) and 20 individual clones from each sample were cycle sequenced by the BigDye Terminator kit (ver. 3.1; Applied Biosystems) and the ABI automated DNA sequencer (Applied Biosystems). Primers used: Fxpro-met_F1, 5′-TTTTTGTGGTGAGGGGAAGAAATTATATT-3′; Fxpro-met_R2, 5′-TACCATCTCCTCCAATAAAACCCACATC-3′; Fxint-met_F8, 5′-TTTGGGTTAAGTTTGTTGTAGGATAGGGTAGTTAG-3′; Fxint-met_R7, 5′-AAATCTACATCTAAACCCTATTATCACAACCCC-3′.

### Single Cell Sorting, RT-PCR, and Vβ5 Sequence Analysis

PBLs were stained with anti-human CD4-FITC, anti-human CD25-PC7 (BD Biosciences), and anti-human BV5.1, BV5.2, BV5.3-PPE (Beckman Coulter). Single cells were sorted with the FACS Vantage (Becton Dickinson) into 96-well PCR plates (Abgene, Epsom). Single-cell RT-PCR conditions were as previously described (Miyara et al., 2006). In the first PCR round, BV5ext (5′-GATCAAAACGAGAGGACAGC-3′) and BC (5′-CGGGCTGCTCCTTGAGGGGCTGCG-3′) were used. Reactions were subjected after 5 min at 94°C to 8 cycles (94°C for 30 s, 60°C for 40 s, 72°C for 50 s), 32 cycles (94°C for 30 s, 55°C for 40 s, 72°C for 50 s), and a final elongation at 72°C for 5 min. In a second PCR round, nested primers BV5 (5′-AGCTCTGAGCTGAATGTGAACGCC-3′) and BC-int (5′-GCGGGTCYGTGCTGACCC-3′) were used. PCR was performed as in the first step.

Products were subjected to automated sequencing (ABI 3100, Applied Biosystems).

Specific questions regarding this repertoire analysis should be sent to guy.gorochov@upmc.fr.

### Microarray and Real-Time PCR

RNA was extracted from FACS-sorted $CD4^+$ T cells according to their amounts of CD25 and CD45RA and analyzed by Affymetrix Human Genome U133 Plus 2.0 Arrays.

Real-time PCR was performed with a SYBR green assay on the LightCycler 480 system (Roche). Total RNA extracted from FACS-sorted T cells was reverse transcribed according to the manufacturer's instructions (RNeasy Micro kit, QIAGEN). In each reaction, hypoxanthine phosphoribosyltransferase-1 (HPRT-1) was amplified as a housekeeping gene to calculate a standard curve and to correct for variations in target sample quantities. Relative copy numbers were calculated for each sample from the standard curve after normalization to HPRT-1 by the instrument software. Primers used: FOXP3_F, 5′- CAGCACATTCCCAGAGTTCC-3′; FOXP3_R,5′-TGAGCGTGGCGTAGGTGAAAG-3′; RORA_F,5′- TCACCAACGGCGAGACTTC-3′; RORA_R,5′-GGCAAACTCCACCACATACTG-3′; RORC_F,5′-CGCTCCAACATCTTCTCC-3′; RORC_R,5′-CTAACCAGCACCACTTCC-3′; AHR_F,5′-AACAGATGAGGAAGGAACAGAGC-3′; AHR_R,5′-GAGTGGATGTGGTAGCAGAGTC-3′; AHRR_F,5′-AAGGCTGCTGTTGGAGTC-3′; AHRR_R,5′- TGGATGTAGTCATAAATGTTCTGG-3′; HPRT-1_F,5′-GCTGAGGATTTGGAAAGGGTG-3′; HPRT-1_R,5′-TGAGCACACAGAGGGCTACAATG-3′.

### ACCESSION NUMBERS

Microarray data are available from the National Center for Biotechnology Information Gene Expression Omnibus (GEO) under accession number GSE15659.

### SUPPLEMENTAL DATA

Supplemental Data include ten figures and two tables and can be found with this article online at http://www.cell.com/immunity/supplemental/S1074-7613(09)00202-7.

### ACKNOWLEDGMENTS

This work was supported by grant in aid from the Ministry of Education, Sports, and Culture of Japan. M.M. was successively supported by la Fondation pour la Recherche Médicale and by Japan Society for the Promotion of Science. The study was also in part supported by a grant from the European Union (ATTACK project LHS-CT-2005-018914). We thank the blood donors and the patients who participated in the study, R. Ishii for expertise in cell sorting, M. Kakino for assistance in molecular biology, M. Yoshida for maintaining mice, and S. Teradaira, A. Kishi, M. Hashimoto, S. Maeda, H. Uryu, K. Hirota, C. Badoual, and N. Sakaguchi for technical help and valuable discussion.

Received: December 25, 2008
Revised: February 23, 2009
Accepted: March 26, 2009
Published online: May 21, 2009

### REFERENCES

Allan, S.E., Crome, S.Q., Crellin, N.K., Passerini, L., Steiner, T.S., Bacchetta, R., Roncarolo, M.G., and Levings, M.K. (2007). Activation-induced FOXP3 in human T effector cells does not suppress proliferation or cytokine production. Int. Immunol. *19*, 345–354.

Baecher-Allan, C., Brown, J.A., Freeman, G.J., and Hafler, D.A. (2001). CD4+CD25high regulatory cells in human peripheral blood. J. Immunol. *167*, 1245–1253.

Baecher-Allan, C., Wolf, E., and Hafler, D.A. (2006). MHC class II expression identifies functionally distinct human regulatory T cells. J. Immunol. *176*, 4622–4631.

Baron, U., Floess, S., Wieczorek, G., Baumann, K., Grutzkau, A., Dong, J., Thiel, A., Boeld, T.J., Hoffmann, P., Edinger, M., et al. (2007). DNA demethylation in the human FOXP3 locus discriminates regulatory T cells from activated FOXP3(+) conventional T cells. Eur. J. Immunol. *37*, 2378–2389.

Curiel, T.J., Coukos, G., Zou, L., Alvarez, X., Cheng, P., Mottram, P., Evdemon-Hogan, M., Conejo-Garcia, J.R., Zhang, L., Burow, M., et al. (2004). Specific recruitment of regulatory T cells in ovarian carcinoma fosters immune privilege and predicts reduced survival. Nat. Med. *10*, 942–949.

Dieckmann, D., Plottner, H., Berchtold, S., Berger, T., and Schuler, G. (2001). Ex vivo isolation and characterization of CD4(+)CD25(+) T cells with regulatory properties from human blood. J. Exp. Med. *193*, 1303–1310.

Ehrenstein, M.R., Evans, J.G., Singh, A., Moore, S., Warnes, G., Isenberg, D.A., and Mauri, C. (2004). Compromised function of regulatory T cells in rheumatoid arthritis and reversal by anti-TNFalpha therapy. J. Exp. Med. *200*, 277–285.

Floess, S., Freyer, J., Siewert, C., Baron, U., Olek, S., Polansky, J., Schlawe, K., Chang, H.D., Bopp, T., Schmitt, E., et al. (2007). Epigenetic control of the foxp3 locus in regulatory T cells. PLoS Biol. *5*, e38.

Fontenot, J.D., Gavin, M.A., and Rudensky, A.Y. (2003). Foxp3 programs the development and function of CD4+CD25+ regulatory T cells. Nat. Immunol. *4*, 330–336.

Fritzsching, B., Oberle, N., Pauly, E., Geffers, R., Buer, J., Poschl, J., Krammer, P., Linderkamp, O., and Suri-Payer, E. (2006). Naive regulatory T cells: A novel subpopulation defined by resistance toward CD95L-mediated cell death. Blood *108*, 3371–3378.

Gavin, M.A., Torgerson, T.R., Houston, E., DeRoos, P., Ho, W.Y., Stray-Pedersen, A., Ocheltree, E.L., Greenberg, P.D., Ochs, H.D., and Rudensky, A.Y. (2006). Single-cell analysis of normal and FOXP3-mutant human T cells: FOXP3 expression without regulatory T cell development. Proc. Natl. Acad. Sci. USA *103*, 6659–6664.

Hermiston, M.L., Xu, Z., and Weiss, A. (2003). CD45: A critical regulator of signaling thresholds in immune cells. Annu. Rev. Immunol. *21*, 107–137.

Hiramatsu, H., Nishikomori, R., Heike, T., Ito, M., Kobayashi, K., Katamura, K., and Nakahata, T. (2003). Complete reconstitution of human lymphocytes from cord blood CD34+ cells using the NOD/SCID/gammacnull mice model. Blood *102*, 873–880.

Hoffmann, P., Eder, R., Boeld, T.J., Doser, K., Piseshka, B., Andreesen, R., and Edinger, M. (2006). Only the CD45RA+ subpopulation of CD4+CD25high T cells gives rise to homogeneous regulatory T-cell lines upon in vitro expansion. Blood *108*, 4260–4267.

Hori, S., Nomura, T., and Sakaguchi, S. (2003). Control of regulatory T cell development by the transcription factor Foxp3. Science *299*, 1057–1061.

Ito, T., Hanabuchi, S., Wang, Y.H., Park, W.R., Arima, K., Bover, L., Qin, F.X., Gilliet, M., and Liu, Y.J. (2008). Two functional subsets of FOXP3+ regulatory T cells in human thymus and periphery. Immunity *28*, 870–880.

Ivanov, I.I., McKenzie, B.S., Zhou, L., Tadokoro, C.E., Lepelley, A., Lafaille, J.J., Cua, D.J., and Littman, D.R. (2006). The orphan nuclear receptor RORgammat directs the differentiation program of proinflammatory IL-17+ T helper cells. Cell *126*, 1121–1133.

Janson, P.C., Winerdal, M.E., Marits, P., Thorn, M., Ohlsson, R., and Winqvist, O. (2008). FOXP3 promoter demethylation reveals the committed Treg population in humans. PLoS ONE *3*, e1612.

Jonuleit, H., Schmitt, E., Stassen, M., Tuettenberg, A., Knop, J., and Enk, A.H. (2001). Identification and functional characterization of human CD4(+)CD25(+) T cells with regulatory properties isolated from peripheral blood. J. Exp. Med. *193*, 1285–1294.

Khattri, R., Cox, T., Yasayko, S.A., and Ramsdell, F. (2003). An essential role for Scurfin in CD4+CD25+ T regulatory cells. Nat. Immunol. *4*, 337–342.

Kimmig, S., Przybylski, G.K., Schmidt, C.A., Laurisch, K., Mowes, B., Radbruch, A., and Thiel, A. (2002). Two subsets of naive T helper cells with distinct T cell receptor excision circle content in human adult peripheral blood. J. Exp. Med. *195*, 789–794.

Kriegel, M.A., Lohmann, T., Gabler, C., Blank, N., Kalden, J.R., and Lorenz, H.M. (2004). Defective suppressor function of human CD4+ CD25+ regulatory T cells in autoimmune polyglandular syndrome type II. J. Exp. Med. *199*, 1285–1291.

Levings, M.K., Sangregorio, R., and Roncarolo, M.G. (2001). Human cd25(+)cd4(+) t regulatory cells suppress naive and memory T cell proliferation and can be expanded in vitro without loss of function. J. Exp. Med. *193*, 1295–1302.

Liu, W., Putnam, A.L., Xu-Yu, Z., Szot, G.L., Lee, M.R., Zhu, S., Gottlieb, P.A., Kapranov, P., Gingeras, T.R., Fazekas de St Groth, B., et al. (2006). CD127 expression inversely correlates with FoxP3 and suppressive function of human CD4+ T reg cells. J. Exp. Med. *203*, 1701–1711.

Mantel, P.Y., Ouaked, N., Ruckert, B., Karagiannidis, C., Welz, R., Blaser, K., and Schmidt-Weber, C.B. (2006). Molecular mechanisms underlying FOXP3 induction in human T cells. J. Immunol. *176*, 3593–3602.

Miyara, M., Amoura, Z., Parizot, C., Badoual, C., Dorgham, K., Trad, S., Nochy, D., Debre, P., Piette, J.C., and Gorochov, G. (2005). Global natural regulatory T cell depletion in active systemic lupus erythematosus. J. Immunol. *175*, 8392–8400.

Miyara, M., Amoura, Z., Parizot, C., Badoual, C., Dorgham, K., Trad, S., Kambouchner, M., Valeyre, D., Chapelon-Abric, C., Debre, P., et al. (2006). The immune paradox of sarcoidosis and regulatory T cells. J. Exp. Med. *203*, 359–370.

Ng, W.F., Duggan, P.J., Ponchel, F., Matarese, G., Lombardi, G., Edwards, A.D., Isaacs, J.D., and Lechler, R.I. (2001). Human CD4(+)CD25(+) cells: a naturally occurring population of regulatory T cells. Blood *98*, 2736–2744.

Onishi, Y., Fehervari, Z., Yamaguchi, T., and Sakaguchi, S. (2008). Foxp3+ natural regulatory T cells preferentially form aggregates on dendritic cells in vitro and actively inhibit their maturation. Proc. Natl. Acad. Sci. USA *105*, 10113–10118.

Quintana, F.J., Basso, A.S., Iglesias, A.H., Korn, T., Farez, M.F., Bettelli, E., Caccamo, M., Oukka, M., and Weiner, H.L. (2008). Control of T(reg) and T(H)17 cell differentiation by the aryl hydrocarbon receptor. Nature *453*, 65–71.

Roncador, G., Brown, P.J., Maestre, L., Hue, S., Martinez-Torrecuadrada, J.L., Ling, K.L., Pratap, S., Toms, C., Fox, B.C., Cerundolo, V., et al. (2005). Analysis of FOXP3 protein expression in human CD4+CD25+ regulatory T cells at the single-cell level. Eur. J. Immunol. *35*, 1681–1691.

Sakaguchi, S., Sakaguchi, N., Asano, M., Itoh, M., and Toda, M. (1995). Immunologic self-tolerance maintained by activated T cells expressing IL-2 receptor alpha-chains (CD25). Breakdown of a single mechanism of self-tolerance causes various autoimmune diseases. J. Immunol. *155*, 1151–1164.

Sakaguchi, S., Yamaguchi, T., Nomura, T., and Ono, M. (2008). Regulatory T cells and immune tolerance. Cell *133*, 775–787.

Seddiki, N., Santner-Nanan, B., Martinson, J., Zaunders, J., Sasson, S., Landay, A., Solomon, M., Selby, W., Alexander, S.I., Nanan, R., et al. (2006). Expression of interleukin (IL)-2 and IL-7 receptors discriminates between human regulatory and activated T cells. J. Exp. Med. *203*, 1693–1700.

Taams, L.S., Smith, J., Rustin, M.H., Salmon, M., Poulter, L.W., and Akbar, A.N. (2001). Human anergic/suppressive CD4(+)CD25(+) T cells: a highly differentiated and apoptosis-prone population. Eur. J. Immunol. *31*, 1122–1131.

Taflin, C., Miyara, M., Nochy, D., Valeyre, D., Naccache, J.M., Altare, F., Salek-Peyron, P., Badoual, C., Bruneval, P., Haroche, J., et al. (2009). FoxP3+ regulatory T cells suppress early stages of granuloma formation but have little impact on sarcoidosis lesions. Am. J. Pathol. *174*, 497–508.

Tran, D.Q., Ramsey, H., and Shevach, E.M. (2007). Induction of FOXP3 expression in naive human CD4+FOXP3 T cells by T-cell receptor stimulation is transforming growth factor-{beta} dependent but does not confer a regulatory phenotype. Blood *110*, 2983–2990.

Valmori, D., Merlo, A., Souleimanian, N.E., Hesdorffer, C.S., and Ayyoub, M. (2005). A peripheral circulating compartment of natural naive CD4 Tregs. J. Clin. Invest. *115*, 1953–1962.

Veldhoen, M., Hirota, K., Westendorf, A.M., Buer, J., Dumoutier, L., Renauld, J.C., and Stockinger, B. (2008). The aryl hydrocarbon receptor links T(H)17-cell-mediated autoimmunity to environmental toxins. Nature *453*, 106–109.

Viglietta, V., Baecher-Allan, C., Weiner, H.L., and Hafler, D.A. (2004). Loss of functional suppression by CD4+CD25+ regulatory T cells in patients with multiple sclerosis. J. Exp. Med. *199*, 971–979.

Vrisekoop, N., den Braber, I., de Boer, A.B., Ruiter, A.F., Ackermans, M.T., van der Crabben, S.N., Schrijver, E.H., Spierenburg, G., Sauerwein, H.P., Hazenberg, M.D., et al. (2008). Sparse production but preferential incorporation of recently produced naive T cells in the human peripheral pool. Proc. Natl. Acad. Sci. USA *105*, 6115–6120.

Vukmanovic-Stejic, M., Zhang, Y., Cook, J.E., Fletcher, J.M., McQuaid, A., Masters, J.E., Rustin, M.H., Taams, L.S., Beverley, P.C., Macallan, D.C., and

Akbar, A.N. (2006). Human CD4+ CD25hi Foxp3+ regulatory T cells are derived by rapid turnover of memory populations in vivo. J. Clin. Invest. *116*, 2423–2433.

Wang, J., Ioan-Facsinay, A., van der Voort, E.I., Huizinga, T.W., and Toes, R.E. (2007). Transient expression of FOXP3 in human activated nonregulatory CD4+ T cells. Eur. J. Immunol. *37*, 129–138.

Wing, K., Onishi, Y., Prieto-Martin, P., Yamaguchi, T., Miyara, M., Fehervari, Z., Nomura, T., and Sakaguchi, S. (2008). CTLA-4 control over Foxp3+ regulatory T cell function. Science *322*, 271–275.

Yagi, H., Nomura, T., Nakamura, K., Yamazaki, S., Kitawaki, T., Hori, S., Maeda, M., Onodera, M., Uchiyama, T., Fujii, S., and Sakaguchi, S. (2004). Crucial role of FOXP3 in the development and function of human CD25+CD4+ regulatory T cells. Int. Immunol. *16*, 1643–1656.

Yang, X.O., Nurieva, R., Martinez, G.J., Kang, H.S., Chung, Y., Pappu, B.P., Shah, B., Chang, S.H., Schluns, K.S., Watowich, S.S., et al. (2008a). Molecular antagonism and plasticity of regulatory and inflammatory T cell programs. Immunity *29*, 44–56.

Yang, X.O., Pappu, B.P., Nurieva, R., Akimzhanov, A., Kang, H.S., Chung, Y., Ma, L., Shah, B., Panopoulos, A.D., Schluns, K.S., et al. (2008b). T helper 17 lineage differentiation is programmed by orphan nuclear receptors ROR alpha and ROR gamma. Immunity *28*, 29–39.

Zhou, L., Lopes, J.E., Chong, M.M., Ivanov, I.I., Min, R., Victora, G.D., Shen, Y., Du, J., Rubtsov, Y.P., Rudensky, A.Y., et al. (2008). TGF-beta-induced Foxp3 inhibits T(H)17 cell differentiation by antagonizing RORgammat function. Nature *453*, 236–240.

Zorn, E., Nelson, E.A., Mohseni, M., Porcheray, F., Kim, H., Litsa, D., Bellucci, R., Raderschall, E., Canning, C., Soiffer, R.J., et al. (2006). IL-2 regulates FOXP3 expression in human CD4+CD25+ regulatory T cells through a STAT-dependent mechanism and induces the expansion of these cells in vivo. Blood *108*, 1571–1579.

# Identification of Severe Combined Immunodeficiency by T-Cell Receptor Excision Circles Quantification Using Neonatal Guthrie Cards

Yoichi Morinishi, MD, PhD, Kohsuke Imai, MD, PhD, Noriko Nakagawa, MD, Hiroki Sato, MHSc, Katsuyuki Horiuchi, MD, PhD, Yoshitoshi Ohtsuka, MD, PhD, Yumi Kaneda, MD, Takashi Taga, MD, PhD, Hiroaki Hisakawa, MD, PhD, Ryosuke Miyaji, MD, Mikiya Endo, MD, Tsutomu Oh–ishi, MD, PhD, Yoshiro Kamachi, MD, PhD, Koshi Akahane, MD, Chie Kobayashi, MD, PhD, Masahiro Tsuchida, MD, PhD, Tomohiro Morio, MD, PhD, Yoji Sasahara, MD, PhD, Satoru Kumaki, MD, PhD, Keiko Ishigaki, MD, PhD, Makoto Yoshida, MD, PhD, Tomonari Urabe, MD, Norimoto Kobayashi, MD, PhD, Yuri Okimoto, MD, PhD, Janine Reichenbach, MD, PhD, Yoshiko Hashii, MD, PhD, Yoichiro Tsuji, MD, PhD, Kazuhiro Kogawa, MD, PhD, Seiji Yamaguchi, MD, PhD, Hirokazu Kanegane, MD, PhD, Toshio Miyawaki, MD, PhD, Masafumi Yamada, MD, PhD, Tadashi Ariga, MD, PhD, and Shigeaki Nonoyama, MD, PhD

**Objective** To assess the feasibility of T-cell receptor excision circles (TRECs) quantification for neonatal mass screening of severe combined immunodeficiency (SCID).

**Study design** Real-time PCR based quantification of TRECs for 471 healthy control patients and 18 patients with SCID with various genetic abnormalities (*IL2RG*, *JAK3*, *ADA*, *LIG4*, *RAG1*) were performed, including patients with maternal T-cell engraftment (n = 4) and leaky T cells (n = 3).

**Results** TRECs were detectable in all normal neonatal Guthrie cards (n = 326) at the levels of $10^4$ to $10^5$ copies/$\mu$g DNA. In contrast, TRECs were extremely low in all neonatal Guthrie cards (n = 15) and peripheral blood (n = 14) from patients with SCID, including those with maternal T-cell engraftment or leaky T cells with hypomorphic RAG1 mutations or LIG4 deficiency. There were no false-positive or negative results in this study.

**Conclusion** TRECs quantification can be used as a neonatal mass screening for patients with SCID. *(J Pediatr 2009;155:829-33).*

See related article, p 834

Severe combined immunodeficiency (SCID) is a genetic disorder characterized by the absence of T-cells and adaptive immunity.[1,2] Affected infants usually have severe infections due to opportunistic pathogens in the first months of life. Hematopoietic stem cell transplantation can reconstitute immune function, although severe infections before hematopoietic stem cell transplantation can be fatal to the patients within the first year of life.[3,4] Thus, early diagnosis before the occurrence of severe infection is essential.[5-7]

Four different mechanisms have been identified as a cause of SCID, including purine metabolism defects, defective signaling of the common $\gamma$-chain–dependent cytokine receptors, defective V(D)J recombination, and defective pre-TCR/TCR signaling.[1,2] Although human SCID is caused by mutations of at least 10 different genes, all patients have a characteristic decreased number of newly

| | |
|---|---|
| BCG | Bacillus Calmette-Guérin |
| BMT | Bone marrow transplantation |
| CMV | Cytomegalovirus |
| FISH | Fluorescent in situ hybridization |
| HSCT | Hematopoietic stem cell transplantation |
| PB | Peripheral blood |
| PCR | Polymerase chain reaction |
| sjTRECs | Signal joint TRECs |
| SCID | Severe combined immunodeficiency |
| TCR | T-cell receptor |
| TRECs | T-cell receptor excision circles |
| UCB | Umbilical cord blood |

From the Department of Pediatrics (Y.M., K.I., N.N., K.H., Y.T., K.K., S.N.), National Defense Medical College, Saitama, Japan; the Department of Medical Informatics (K.I., H.S.), National Defense Medical College Hospital, Saitama, Japan; the Department of Pediatrics (Y.O., Y.K.), Hyogo College of Medicine, Hyogo, Japan; Department of Pediatrics (T.T.), Shiga University of Medical Science, Shiga, Japan; the Department of Pediatrics (H.H.), Kochi University, Kochi, Japan; the Department of Pediatrics (R.M.), University of Occupational and Environmental Health, Fukuoka, Japan; the Department of Pediatrics (M.E.), Iwate Medical University, Iwate, Japan; the Division of Infectious Diseases, Immunology, and Allergy (T.O.), Saitama Children's Medical Center, Saitama, Japan; the Department of Pediatrics (Y.K.), Nagoya University Graduate School of Medicine, Aichi, Japan; the Department of Pediatrics (K.A.), Yamanashi Prefectural Central Hospital, Yamanashi, Japan; the Department of Pediatrics (C.K., M.T.), Ibaraki Children's Hospital, Ibaraki, Japan; the Department of Pediatrics (T.M.), Tokyo Medical and Dental University, Tokyo, Japan; the Department of Pediatrics (Y.S., S.K.), Tohoku University, Miyagi, Japan; the Department of Pediatrics (K.I.), Tokyo Women's Medical University, Tokyo, Japan; the Department of Pediatrics (M.Y.), Asahikawa Medical College, Hokkaido, Japan; the Department of Pediatrics (T.U.), Kumamoto University, Kumamoto, Japan; the Department of Interdisciplinary Medicine (N.K.), Nagano Children's Hospital, Nagano, Japan; the Department of Hematology/Oncology (Y.O.), Chiba Children's Hospital, Chiba, Japan; the Department of Immunology/Hematology/BMT (J.R.), University Children's Hospital Zurich, Zurich, Switzerland; the Department of Pediatrics (Y.H.), Osaka University, Osaka, Japan; the Department of Pediatrics (S.Y.), Shimane University, Shimane, Japan; the Department of Pediatrics (H.K., T.M.), University of Toyama, Toyama, Japan; and the Department of Pediatrics (M.Y., T.A.), Hokkaido University, Hokkaido, Japan

Supported by grants from the Ministry of Defense, Ministry of Health, Labour and Welfare Kawano Masanori Foundation for Promotion of Pediatrics, Jeffrey Modell Foundation, and The Mother and Child Health Foundation. The authors declare no conflicts of interest.

 10.1016/j.jpeds.2009.05.026

Table. Genotype, lymphocyte subset, and TRECs of patients with SCID

| Patient | Sex | Genotype | Age at onset of symptoms | Age at SCID diagnosis | Lymphocytes (/μL) | CD3+ (%) | CD3+ (/μL) | CD19+ (%) | CD45RO+ / CD4 + CD3 + (%) | Maternal lymphocyte engraftment | Guthrie cards TRECs (/μg DNA) | PB Pre-HSCT TRECs (/μg DNA) | PB Pre-HSCT Age |
|---|---|---|---|---|---|---|---|---|---|---|---|---|---|
| 1 | M | *IL2RG* | 3 mo | 3 mo | 720 | 0.0 | 0 | - | 86.0 | - | <10 | - | - |
| 2 | M | *IL2RG* | - | 0 mo | 780 | 0.0 | 0 | - | 94.0 | - | <10 | <10 | 0 y, 0 mo |
| 3 | M | *IL2RG* | - | 0 mo | 920 | 0.0 | 0 | - | 91.0 | - | <10 | <10 | 0 y, 0 mo |
| 4 | M | *IL2RG* | 4 mo | 5 mo | 2550 | 0.2 | 5 | NA | 99.4 | - | <10 | <10 | 0 y, 5 mo |
| 5 | M | *IL2RG* | 10 mo | 10 mo | 1035 | 0.0 | 0 | - | 94.7 | - | <10 | <10 | 0 y, 10 mo |
| 6 | M | *IL2RG* | 4 mo | 5 mo | 3560 | 0.0 | 0 | - | 95.8 | - | <10 | <10 | 0 y, 5 mo |
| 7 | M | *IL2RG* | - | 0 mo | 966 | 0.7 | 7 | 95.3 | 77.5 | - | <10 | <10 | 0 y, 0 mo |
| 8 | M | *JAK3* | 4 mo | 4 mo | 3810 | 0.0 | 0 | - | 87.0 | - | <10 | - | - |
| 9 | F | *JAK3* | 2 mo | 5 mo | 2495 | 0.0 | 0 | - | 89.8 | - | <10 | <10 | 0 y, 6 mo |
| 10 | M | *ADA* | 1 mo | 4 mo | 90 | 40.0 | 36 | 99.5 | 4.4 | - | <10 | <10 | 0 y, 2 mo |
| 11 | M | *ADA* | 1 mo | 2 m | 100 | 6.8 | 7 | 89.9 | 0.9 | - | $6.2 \times 10^2$ | <10 | 0 y, 1 mo |
| 12 | M | *IL2RG* | 8 mo | 8 mo | 3250 | 40.8 | 1326 | 89.8 | 65.5 | T + NK+ | - | <10 | 1 y |
| 13 | M | *IL2RG* | - | 0 mo | 950 | 4.2 | 40 | NA | 68.6 | T+ | <10 | - | - |
| 14 | M | *IL2RG* | 9 mo | 10 mo | 860 | 7.0 | 60 | 99.6 | 85.9 | T + NK+ | <10 | <10 | 0 y, 10 mo |
| 15 | M | *IL2RG* | 3 mo | 3 mo | 300 | 36.5 | 110 | NA | 53.5 | T+ | <10 | - | - |
| 16 | F | *LIG4* | - | 0 mo | 550 | 38.7 | 213 | 97.6 | 0.3 | - | - | <10 | 2 y |
| 17 | M | *LIG4* | 1 y, 6 mo | 4 y | 300 | 44.3 | 133 | 25.2 | 0.1 | - | <10 | <10 | 4 y |
| 18 | F | *RAG1* | 8 mo | 1 y 9 mo | 550 | 53.1 | 292 | 91.6 | 12.0 | - | - | $8.0 \times 10^1$ | 2 y |

NA, Not available.

developed T cells.[1,2,8,9] T-cell receptor excision circles (TRECs) are small circular DNA fragments formed through rearrangement of the T-cell receptor (TCR) $\alpha$ locus and do not multiply during cell division.[9-13] Therefore, TRECs quantification is reportedly useful for determining recent thymic emigrants. Two reports of a method for neonatal screening of SCID using TRECs quantification by real-time PCR have been published.[6,7] Both studies quantified TRECs of patients with SCID using peripheral blood and found significantly lower levels of TRECs than those of control neonates. In addition, Guthrie cards from 2 patients with SCID retrospectively had undetectable TRECs.[6] Most control neonates had high amounts of TRECs. However, TRECs were undetectable in some samples. To increase specificity, 1 study[7] proposed a 2-tiered strategy using a combination of quantified TRECs and IL-7.

We have evaluated blood from Guthrie cards and peripheral blood from control patients and patients with SCID for detecting TRECs.

## Methods

Peripheral blood samples were obtained from 112 healthy volunteers (median age, 14 years; range, 0.1 to 51 years). Thirty-three umbilical cord blood samples (median gestational age, 38.9 weeks) were collected at the National Defense Medical College Hospital. Dried blood spots of umbilical cord blood were obtained by applying 50 $\mu$L of residual blood to the 11-mm circles on filter-paper cards (PKU-S, Toyoroshi, Tokyo, Japan). Twenty-six neonatal Guthrie cards with dried blood spots were donated from surplus routine samples for newborn mass screening from neonates born at National Defense Medical College Hospital during this study period (January 2005 to December 2007). In addition, 300 neonatal Guthrie cards, stored at −20°C for less than 5 years in a neonatal mass screening center at Shimane University, were analyzed.

Eighteen patients with SCID were analyzed for TRECs (**Table**). All patients were genetically diagnosed using genomic DNA sequencing. Mutations of either *IL2RG* (n = 11), *JAK3* (n = 2), *RAG1* (n = 1), *ADA* (n = 2), or *LIG4* (n = 2) were identified in the patients (**Table**).

Peripheral blood samples of 14 patients before hematopoietic stem cell transplantation were used. In addition, neonatal Guthrie cards of 15 patients that had been stored in newborn mass screening centers were obtained.

Maternal T and NK lymphocyte engraftment was diagnosed by fluorescent in situ hybridization (FISH) using X and Y chromosome–specific probes after purification of each compartment by specific monoclonal antibodies and immunomagnetic beads.

The study protocol was approved by the National Defense Medical College Institutional Review Board, and informed consent was obtained from the parents of patients with SCID and healthy control patients, as well as adult control patients, in accordance with the Declaration of Helsinki.

### Quantification of TRECs by Real-Time PCR

We used 100 $\mu$L of whole blood (EDTA anticoagulated peripheral blood and heparinized cord blood) or 2 punches of 6 mm in diameter from Guthrie card to extract genomic DNA.

Concentrations of DNA from peripheral blood, fresh dried blood punches from normal neonates (n = 26), and stored dried blood spots from normal neonates (n = 300) were

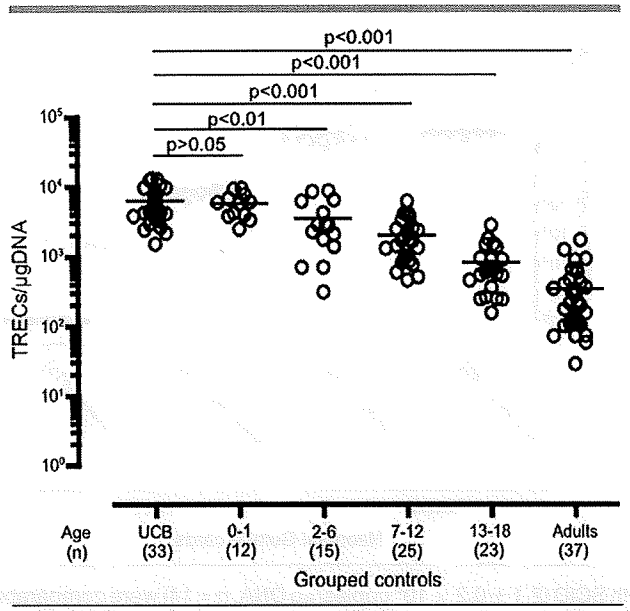


**Figure 1.** Umbilical cord blood (UCB) (n = 33) and peripheral blood (n = 112, 0 to 51 years) samples were analyzed. TRECs in different age groups are shown. TRECs were significantly higher in umbilical cord blood ($6.2 \pm 3.2 \times 10^3$ copies/$\mu$g DNA) and infants ($5.8 \pm 2.3 \times 10^3$ copies/$\mu$g DNA) as compared with other age groups of children ($3.5 \pm 2.8 \times 10^3$ copies/$\mu$g DNA in 2 to 6 years old, $2.0 \pm 1.4 \times 10^3$ copies/$\mu$g DNA in 7 to 12 years old, $8.2 \pm 6.3 \times 10^2$ copies/$\mu$g DNA in 13 to 18 years old) and adults ($3.4 \pm 3.6 \times 10^2$ copies/$\mu$g DNA).

$40.6 \pm 2.3$ ng/$\mu$L (mean $\pm$ SEM) (range, 13 to 167 ng/$\mu$L), $7.8 \pm 2.8$ ng/$\mu$L (2.9 to 13.0 ng/$\mu$L), and $5.3 \pm 0.2$ ng/$\mu$L (0.6 to 20.2 ng/$\mu$L), respectively.

Quantitative real-time PCR for $\delta$Rec-$\psi J\alpha$ sjTRECs was performed using the same primers and $\delta$Rec probes as reported by Hazenberg et al.[14]

As an internal control, RNaseP gene was amplified in each sample tested using TaqMan RNaseP Primer-Probe (VIC dye) Mix (Applied Biosystems, Foster City, California).

### Statistical Analysis

An exponential regression model was used to quantify the relationship between age and TRECs levels (per $\mu$g DNA and per RNaseP). Goodness-of-fit of the model was evaluated by $R^2$. The Dunnett multiple comparison test was conducted to test the differences of each age group (0 to 1, 2 to 6, 7 to 12, 13 to 18 years and adults) versus umbilical cord blood comparisons serving as a control group (**Figure 1**). RNaseP and TRECs levels of patients with SCID and control patients were compared by an unpaired Student $t$ test (if the variance was equal) or Welch $t$ test (if the variance was different).

All statistical analyses were performed using GraphPad Prism Version 4.00 (GraphPad Software, San Diego, California). $P < .05$ denotes a statistically significant difference.

## Results

TRECs were detectable in all DNA samples from whole blood of normal control patients, including umbilical cord blood (n = 33), healthy infants (0 to 1 year old, n = 12), children (2 to 18 years old, n = 63), and adults (n = 37). TRECs in whole blood were found to decline with increasing age ($r = 0.851$). TRECs of umbilical cord blood were significantly higher than those of children and adults but were not significantly different from those of infants (**Figure 1**). We found a strong correlation between TRECs copies/$\mu$g DNA and TRECs/RNaseP ratio ($r = 0.979$).

TRECs of peripheral blood samples from all 14 patients with SCID before hematopoietic stem cell transplantation were below detectable levels (<10 copies/$\mu$g DNA) with the exception of 1 (P18, see below), in contrast to high levels of control infants ($5.8 \pm 0.7 \times 10^3$/$\mu$g DNA, n = 12) ($P < .0001$) (**Figure 2**, A).

Next, we analyzed TRECs of dried blood spots from normal control neonates using simulated Guthrie cards from cord blood (n = 31), neonatal Guthrie cards obtained during this study period (January 2005 to December 2007) (n = 26), and those stored in a neonatal mass screening center for less than 5 years (n = 300). TRECs were detectable in all dried blood spots: in cord blood ($1.3 \pm 0.1 \times 10^4$ copies/$\mu$g DNA, mean $\pm$ SEM), in neonatal Guthrie cards ($2.3 \pm 0.2 \times 10^4$ copies/$\mu$g DNA), and in stored neonatal Guthrie cards ($3.6 \pm 0.2 \times 10^5$ copies/$\mu$g DNA).

To determine whether this method can identify patients with SCID, we quantified TRECs using 15 stored neonatal Guthrie cards from patients with SCID (patients 1 through 11, 13 through 15, and patient 17). RNaseP levels were high in all neonatal Guthrie cards from patients with SCID ($1.8 \pm 0.3 \times 10^6$ copies/$\mu$g DNA, n = 15), which were similar to control levels ($2.3 \pm 0.1 \times 10^6$ copies/$\mu$g DNA, n = 26) ($P = .184$), indicating an appropriate amount of genomic DNA was extracted from the neonatal Guthrie cards (**Figure 2**, B). In contrast, TRECs were below detection levels in all patients ($P < .0001$) except 1 (patient 11). This patient with SCID had compound heterozygous mutations of *ADA* (Gln119Stop/Arg34Ser). He had detectable but significantly lower levels of TRECs ($6.2 \times 10^2$ copies/$\mu$g DNA) than those of control neonates ($2.3 \pm 0.2 \times 10^4$ copies/$\mu$g DNA, n = 26) (**Figure 2**, B). At 1 month of age, the TRECs from the peripheral blood of patient 11 were below detectable levels (**Table** and **Figure 2**, A).

These results indicate that neonatal mass screening of SCID by quantitative real-time PCR for TRECs using neonatal Guthrie cards is feasible.

We analyzed TRECs in 4 patients with SCID with maternal T-cell engraftment (patients 12 through 15, $CD3^+$ cells: 40 to 1326/$\mu$L). We found that all patients had undetectable levels of TRECs in neonatal Guthrie cards (patients 13 through 15) and peripheral blood (patients 12 and 14). Patient 12 had a normal lymphocyte count (3250/$\mu$L) on admission as well as a significant number of T, B, and NK cells (**Table**). His peripheral blood TRECs level was below the detection

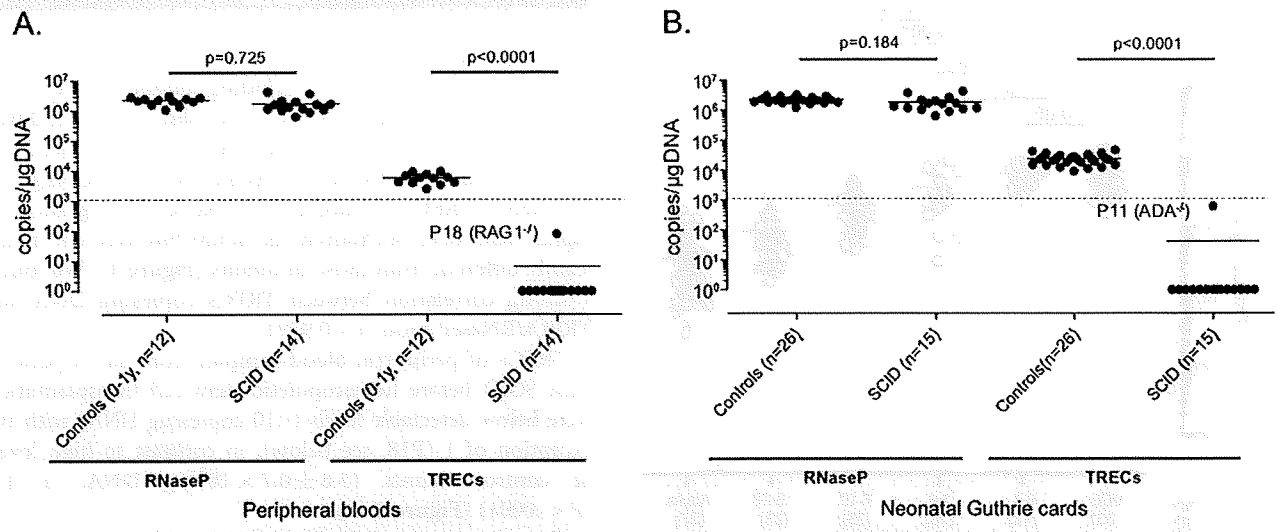


**Figure 2. A,** RNaseP levels in peripheral blood from patients with SCID ($2.1 \pm 0.2 \times 10^6$ copies/$\mu$g DNA, n = 14) were comparable with those from control infants ($2.2 \pm 0.2 \times 10^6$ copies/$\mu$g DNA, n = 12) ($P = .725$). Peripheral blood TRECs from all typical patients with SCID were undetectable (<10 copies/$\mu$g DNA) as compared with the high copy number of peripheral blood TRECs from control neonates ($5.8 \pm 0.7 \times 10^3$ copies/$\mu$g DNA, n = 12) ($P < .0001$). Patient 18, with hypomorphic RAG1 mutations, had detectable but extremely low TRECs in peripheral blood ($8.0 \times 10^1$ copies/$\mu$g DNA). **B,** RNaseP levels in neonatal Guthrie cards from patients with SCID ($1.8 \pm 0.3 \times 10^6$ copies/$\mu$g DNA, n = 15) were comparable with those from control neonates ($2.3 \pm 0.1 \times 10^6$ copies/$\mu$g DNA, n = 26) ($P = .184$). TRECs of Guthrie cards from 14 of 15 patients with SCID during the early neonatal period were undetectable (<10 copies/$\mu$g DNA). An ADA-deficient patient ($ADA^{-/-}$, patient 11) had detectable but significantly low TRECs levels ($6.2 \times 10^2$ copies/$\mu$g DNA) compared with control neonates ($2.3 \pm 0.2 \times 10^4$ copies/$\mu$g DNA, n = 26).

levels despite the presence of peripheral T cells. FISH analysis revealed that all circulating $CD3^+$ cells (1326/$\mu$L) were derived from his mother. Similarly, TRECs of other patients (patients 13 through 15) were also undetectable despite the maternal T cells (**Table**).

These results confirm the findings of Patel et al[9] indicating that TRECs quantification is both effective and reliable for the screening of SCID even in the presence of maternal T cells.

Patient 18 with hypomorphic *RAG1* mutations was lymphopenic (550/$\mu$L) at 21 months of age, but T (53.1%), B (12.0%), and NK cells (31.2%) were present in peripheral blood. Both T cells with TCR$\alpha\beta$ chain and TCR$\gamma\delta$ chain were derived from the patient, as determined by FISH analysis of the sex chromosome.

The peripheral blood TRECs from this patient ($8.0 \times 10^1$ copies/$\mu$g DNA) (**Figure 2**, A) was significantly lower than age-matched control patients ($5.2 \pm 3.2 \times 10^3$ copies/$\mu$g DNA, n = 5). We purified T cells with TCR$\alpha\beta$ chain by FACS sorting. T cells with TCR$\alpha\beta$ from patient 18 had very low TRECs/cells ($4.0 \times 10^1$ copies/$10^5$ cells) than those of age-matched control patients ($5.1 \times 10^3$ copies/$10^5$ cells).

We also analyzed TRECs in 2 LIG4-deficient patients (patients 16 and 17) who had leaky T cells (**Table**). Peripheral blood TRECs were undetectable in both patients (**Figure 2**, A), and TRECs in the neonatal Guthrie card were also undetectable in patient 17 (**Figure 2**, B).

These results indicate that TRECs are extremely low in patients with SCID, even if leaky T cells are present.

## Discussion

We demonstrated that TRECs were undetectable, or were significantly lower ($10^1$ to $10^2$ copies/$\mu$g DNA) than healthy neonates and infants ($10^4$ to $10^5$ copies/$\mu$g DNA), in both neonatal Guthrie cards and peripheral blood samples obtained from SCID. All types of SCID tested, including IL2RG, JAK3, ADA, RAG1, LIG4 deficiencies, were identified by measuring TRECs. This finding was consistent with the previous reports that showed the usefulness of TRECs for the identification of SCID[6,7,9] and further indicates that TRECs can identify SCID with maternal T cells and SCID with leaky T cells. In 2 LIG4-deficient patients with leaky T cells (CD3 + 38.7% and 44.3%) and in 1 patient with hypomorphic mutations in *RAG1* gene, who had immunodeficiency and autoimmunity with residual memory T cells,[15,16] TRECs were undetectable. These results indicate that TRECs is a good marker to identify the defect of V(D)J recombination, in which LIG4 and RAG1 play essential roles. We observed progressive loss of TRECs in a patient with SCID and ADA deficiency (patient 11). This observation is compatible with the report that the loss of naive T lymphocytes occurs after birth in patients with ADA deficiency.[17,18]

No false-negative was observed in this study (TRECs were below normal range in all cases of SCID), although sample size was too small to determine the exact false-negative rate.

Consistently, there were no false-positive (TRECs were all positive) in the control samples in this study. The previous studies showed 2.9% and 7.7% of false-positive rates.[6,7] The primers and probe used in this study [14] were different from previously studies.[6,7] However, both probes were found to result in equivalent quantities (data not shown). Thus, the reason of the different false-positive rate between this and the previous studies is currently undetermined. Mass screening using larger population will disclose the exact false-positive and false-negative rate.

The cost to test 1 sample in our study is $5 per sample, which was reported to be cost-effective.[19] We are now trying to further reduce the cost.

Early diagnosis of SCID can prevent severe and recurrent infection, which is often fatal and makes stem cell transplantation difficult. Identification of SCID by newborn screening by TRECs will improve the prognosis and quality of life of patients with SCID. ■

*We thank the patients and their families who participated in this study. We also thank Mrs Makiko Tanaka for her skillful technical assistance and members of Department of Obstetrics and Gynecology, National Defense Medical College for collecting umbilical cord blood samples.*

Submitted for publication Oct 10, 2008; last revision received April 22, 2009; accepted May 19, 2009.

Reprint requests: Dr Kohsuke Imai, National Defense Medical College, 3-2 Namiki, Tokorozawa, Saitama, Japan, 359-8513. E-mail: kimai@ndmc.ac.jp.

## References

1. Fischer A, Le Deist F, Hacein-Bey-Abina S, Andre-Schmutz I, BasileGde S, de Villartay JP, et al. Severe combined immunodeficiency: a model disease for molecular immunology and therapy. Immunol Rev 2005;203:98-109.
2. Buckley RH. Molecular defects in human severe combined immunodeficiency and approaches to immune reconstitution. Annu Rev Immunol 2004;22:625-55.
3. Buckley RH, Schiff SE, Schiff RI, Markert L, Williams LW, Roberts JL, et al. Hematopoietic stem-cell transplantation for the treatment of severe combined immunodeficiency. N Engl J Med 1999;340:508-16.
4. Antoine C, Muller S, Cant A, Cavazzana-Calvo M, Veys P, Vossen J, et al. Long-term survival and transplantation of haemopoietic stem cells for immunodeficiencies: report of the European experience 1968-99. Lancet 2003;361:553-60.
5. Myers LA, Patel DD, Puck JM, Buckley RH. Hematopoietic stem cell transplantation for severe combined immunodeficiency in the neonatal period leads to superior thymic output and improved survival. Blood 2002;99:872-8.
6. Chan K, Puck JM. Development of population-based newborn screening for severe combined immunodeficiency. J Allergy Clin Immunol 2005; 115:391-8.
7. McGhee SA, Stiehm ER, Cowan M, Krogstad P, McCabe ER. Two-tiered universal newborn screening strategy for severe combined immunodeficiency. Mol Genet Metab 2005;86:427-30.
8. Buckley RH, Schiff RI, Schiff SE, Markert ML, Williams LW, Harville TO, et al. Human severe combined immunodeficiency: genetic, phenotypic, and functional diversity in one hundred eight infants. J Pediatr 1997;130:378-87.
9. Patel DD, Gooding ME, Parrott RE, Curtis KM, Haynes BF, Buckley RH. Thymic function after hematopoietic stem-cell transplantation for the treatment of severe combined immunodeficiency. N Engl J Med 2000; 342:1325-32.
10. de Villartay JP, Hockett RD, Coran D, Korsmeyer SJ, Cohen DI. Deletion of the human T-cell receptor delta-gene by a site-specific recombination. Nature 1988;335:170-4.
11. Douek DC, McFarland RD, Keiser PH, Gage EA, Massey JM, Haynes BF, et al. Changes in thymic function with age and during the treatment of HIV infection. Nature 1998;396:690-5.
12. McFarland RD, Douek DC, Koup RA, Picker LJ. Identification of a human recent thymic emigrant phenotype. Proc Natl Acad Sci U S A 2000;97:4215-20.
13. Hazenberg MD, Verschuren MC, Hamann D, Miedema F, van Dongen JJ. T cell receptor excision circles as markers for recent thymic emigrants: basic aspects, technical approach, and guidelines for interpretation. J Mol Med 2001;79:631-40.
14. Hazenberg MD, Otto SA, CohenStuart JW, Verschuren MC, Borleffs JC, Boucher CA, et al. Increased cell division but not thymic dysfunction rapidly affects the T-cell receptor excision circle content of the naive T cell population in HIV-1 infection. Nat Med 2000;6: 1036-42.
15. de Villartay JP, Lim A, Al-Mousa H, Dupont S, Dechanet-Merville J, Coumau-Gatbois E, et al. A novel immunodeficiency associated with hypomorphic RAG1 mutations and CMV infection. J Clin Invest 2005;115: 3291-9.
16. Ehl S, Schwarz K, Enders A, Duffner U, Pannicke U, Kuhr J, et al. A variant of SCID with specific immune responses and predominance of gamma delta T cells. J Clin Invest 2005;115:3140-8.
17. Giblett ER, Anderson JE, Cohen F, Pollara B, Meuwissen HJ. Adenosine-deaminase deficiency in two patients with severely impaired cellular immunity. Lancet 1972;2:1067-9.
18. Hershfield MS. Genotype is an important determinant of phenotype in adenosine deaminase deficiency. Curr Opin Immunol 2003;15:571-7.
19. McGhee SA, Stiehm ER, McCabe ER. Potential costs and benefits of newborn screening for severe combined immunodeficiency. J Pediatr 2005; 147:603-8.

European Journal of Haematology ISSN 0902-4441

ORIGINAL ARTICLE

# Possible application of flow cytometry for evaluation of the structure and functional status of WASP in peripheral blood mononuclear cells

Masaru Nakajima[1,3], Masafumi Yamada[2], Koji Yamaguchi[3], Yukio Sakiyama[3], Atsushi Oda[4], David L. Nelson[5], Yasutaka Yawaka[1], Tadashi Ariga[2]

[1]Division of Oral Functional Science, Department of Dentistry for Children and Disabled Person, Hokkaido University Graduate School of Dental Medicine, Sapporo, Japan; [2]Department of Pediatrics, Hokkaido University Graduate School of Medicine, Sapporo, Japan; [3]Research Group of Human Gene Therapy, Hokkaido University, Graduate School of Medicine, Sapporo, Japan; [4]Department of Preventive Medicine, Hokkaido University School of Medicine, Sapporo, Japan; [5]National Institutes of Health, National Cancer Institute, Metabolism Branch, Bethesda, MD, USA

## Abstract

The Wiskott-Aldrich syndrome protein (WASP), which is defective in Wiskott-Aldrich syndrome (WAS) patients, is an intracellular protein expressed in non-erythroid hematopoietic cells. Previously, we have established methods to detect intracellular WASP expression in peripheral blood mononuclear cells (PBMNCs) using flow cytometric analysis (FCM-WASP) and have revealed that WAS patients showed absent or very low level intracellular WASP expression in lymphocytes and monocytes, while a significant amount of WASP was detected in those of normal individuals. We applied these methods for diagnostic screening of WAS patients and WAS carriers, as well as to the evaluation of mixed chimera in WAS patients who had previously undergone hematopoietic stem cell transplantation. During these procedures, we have noticed that lymphocytes from normal control individuals showed dual positive peaks, while their monocytes invariably showed a single sharp WASP-positive peak. To investigate the basis of the dual positive peaks ($WASP^{low\text{-}bright}$ and $WASP^{high\text{-}bright}$), we characterized the constituent linage lymphocytes of these two WASP-positive populations. As a result, we found each $WASP^{low/high}$ population comprised different linage PBMNCs. Furthermore, we propose that the difference between the two WASP-positive peaks did not result from any difference in WASP expression in the cells, but rather from a difference in the structural and functional status of the WASP protein in the cells. It has been shown that WASP may exist in two forms; an activated or inactivated form. Thus, the structural and functional WASP status or configuration could be evaluated by flow cytometric analysis.

**Key words** Wiskott-Aldrich syndrome protein; flow cytometry; Wiskott-Aldrich syndrome; peripheral blood mononuclear cells

**Correspondence** Tadashi Ariga, Department of Pediatrics, Hokkaido University Graduate School of Medicine, Japan. Tel: +81-11-706-7153; Fax: +81-11-706-7898; e-mail: tada-ari@med.hokudai.ac.jp

Accepted for publication 19 October 2008

doi:10.1111/j.1600-0609.2008.01180.x

The Wiskott-Aldrich syndrome protein (WASP) is the causative molecule underlying WAS (1). WASP comprises 502 amino acid residues, and is encoded by the *WASP gene*, which is organized into 12 exons encompassing 9 kb gDNA, and is located on the X-chromosome at Xp11.23-p11.22 (2). WASP belongs to the growing family of WASP/Scar/WAVE cytoplasmic scaffolding proteins, which are involved in cytoskeleton remodeling and actin nucleation/polymerization in response to activation stimuli (3, 4). Recent studies have revealed that WASP interacts with a number of intracellular molecules and plays key roles in signal transduction and the regulation of actin-polymerization (5–9). Furthermore, on the basis of crystal structure studies of the WASP molecule, it has been shown that WASP is involved in an auto-inhibition and activation mechanism via intra-molecular conformation changes (10).

Loss of function mutations in the *WASP* genes causes WAS, and X-linked thrombocytopenia (XLT) (11, 12), while gain of function mutations in the WASP gene have shown to cause X-linked neutropenia (XLN) (13). However, the full extent of the varied clinical symptoms observed in these patients (14–20) has not been fully elucidated in relation to WASP abnormalities.

Previously, we have established methods to detect intracellular WASP expression in peripheral blood mononuclear cells (PBMNCs) by flow cytometric analysis (FCM-WASP) (21). We have applied the methods to the screening of WAS patients, for the identification of carrier (22–24), or for the evaluation of WAS patients after receiving hematopoietic stem cell transplantation (25) and finally to detection of spontaneous reversion of WAS cases (26). During these pervious FCM-WASP experiments, we have identified normal control individual lymphocytes that showed dual positive peaks (WASP$^{low\text{-}bright}$ and WASP$^{high\text{-}bright}$). In this study, we tried to characterize the constituent cell lineage members of these two distinct populations of normal lymphocytes as detected by FCM-WASP, and investigate the mechanism underlying the two populations. Here we demonstrate that the two WASP populations consist of different lineage lymphocytes, and the difference between the two WASP$^{low/high}$ lymphocyte populations seems to result from differences in the functional status of the WASP molecule in the cell.

## Materials and methods

### Anti-WASP antibodies

Two different anti-WASP antibodies were used in this study. One is 3F3A5 (1.2 mg/mL), unconjugated mouse-IgG1 monoclonal anti-WASP antibody (11), which was raised against recombinant WASP corresponding to amino acids 202–302. We used 3F3A5 for FCM-WASP with fluorescein isothiocyanate (FITC)-conjugated goat anti-mouse IgG1 antibody (Southern Biotechnology Associates, Birmingham, AL, USA, 1.0 mg/mL). The second antibody was B-9 (Santa Cruz Biotechnology, Inc, 200 $\mu$g/mL), a phycoerythrin (PE)-conjugated mouse monoclonal IgG2a antibody, which was raised against recombinant WASP corresponding to amino acids 1–250.

### FCM-WASP

FCM-WASP was performed as previously described (21). In brief, PBMNCs were purified using Ficoll-Hypaque, and both the cell surface and cytoplasm were stained. For staining cytoplasmic WASP, cells were treated with Cytofix/Cytoperm solution from the CytoStain kit (Pharmingen, San Diego, CA, USA) at 4°C for 20 min. After two washes with Perm/Wash solution (Pharmingen), they were incubated with 200× diluted mouse anti-WASP antibody (3F3A5) or 5× diluted mouse IgG1 antibody (BectonDickinson, San Jose, CA, USA) at 4°C for 30 min. After washing in phosphate-buffer saline (PBS)-2% fetal bovine serum (P-2), they were incubated with 100× diluted goat anti-mouse IgG1-FITC antibody (Southern Biotechnology Associates) as the secondary antibody again at 4°C for 30 min. In some experiments, a second, 10× diluted different anti-WASP antibody (B-9) was used. We used 10× diluted PE-conjugated mouse IgG2 as an isotypic control antibody. For surface/intracellular dual staining using the 3F3A5 antibody, we first stained the cell surface, followed by washing twice before performing intracellular staining. Antibodies used for surface staining were as follows; 5 $\mu$L of PE-conjugated anti-CD4, 10 $\mu$L of anti-CD8, and 10 $\mu$L of anti-CD56 (Southern Biotechnology Associates); PE-conjugated 10 $\mu$L of anti-CD20 (Beckman Coulter, Fullerton, CA, USA); and 10 $\mu$L of PE-Cy5-conjugated anti-CD45RA and 10 $\mu$L of anti-CD45RO (eBioscience, San Diego, CA, USA). The antibodies or the cell surface staining were mouse IgG2 to avoid cross reactivity with the 100× diluted goat anti-mouse IgG1-FITC antibody. We washed it with P-2 twice and stained intracellular WASP as described above. Stained PBMNCs were analyzed by FACSCalibur (BD, San Jose, CA, USA), using CellQuest software (Becton Dickinson).

### Simultaneous staining with the two anti-WASP antibodies

After fixation and permeabilization procedure, normal control individual lymphocytes were simultaneously stained with 3F3A5 and B-9 at 4°C for 30 min, followed by staining with goat anti-mouse IgG1-FITC, and then, FCM-WASP was performed. The two WASP antibodies were used at the same protein concentration.

### CD3+/CD45RA+ and CD3+/CD45RO+ purification

The two populations of CD3+/CD45RA+ and CD3+/CD45RO+ were purified as follows. Twenty microliters of CD3, CD45RA or CD45RO MicroBeads (Miltenyi Biotec, Bergisch Gladbach, Germany) diluted with 80 $\mu$L of magnetic cell sorting (MACS) buffer (pH 7.2, PBS 0.5% BSA, 2 mM EDTA) were incubated with each batch of $10^7$ lymphocytes at 4°C for 15 min, and then, these cells were washed in MACS buffer. Afterwards, the two populations prepared as above were separated with Vario MACS (Miltenyi Biotec) and an MS

column (Miltenyi Biotec). Each cell population was checked for purity by flow cytometry.

### Western blot analysis

The CD3+CD45RA+ ($WASP^{low\text{-}bright}$) lineages and CD3+CD45RO+ ($WASP^{high\text{-}bright}$) cells were respectively dissolved in RIPA buffer (Sigma, St Louis, MO, USA) containing protease inhibitors at 4°C for 20 min and were centrifuged at 14 500 *g* at 4°C for 20 min. We completely dissolved the cells in SD sample buffer (Sigma) and after boiling the samples, the cell extract of comprising $5 \times 10^6$ equivalency was electrophoresed with 10% polyacrylamide gel and blotted on a Hybond-PPVDF membrane (Amersham, Buckinghamshire, UK). We then stained the membrane with 1000× diluted 3F3A5 and 250× diluted anti-WIP antibody (kindly provided by Dr Ramesh N, Children's Hospital, Harvard University, MA, USA) as a loading control, followed by 1000× diluted peroxidase-conjugated goat anti-mouse IgG and 1000× diluted peroxidase-conjugated goat anti-rabbit IgG, and then used the ECL detection system (Amersham, Aylesbury, UK) for the detection of bands.

### RT-PCR analysis

Total RNA from CD3+CD45RA+cells or CD3+CD45RO+ cells was extracted using an RNA isolation solvent (RNA zolTM Cinna/Biotecx, Houston, TX, USA). Two micrograms each of total RNA was used for cDNA synthesis with the first-strand cDNA synthesis kit (Pharmacia LKB Biotechnology, Uppsala, Sweden) and then, the same volume of each part of cDNA product was PCR-amplified with a set of primers (forward: GAAGACAAGGGCAGAAAGCA, reverse: GGGTTATCCTTCACGAAGCA). We performed electrophoresis of the PCR products and photographed the bands stained with ethidium bromide in the gel under ultraviolet light.

### FCM-WASP for CD8+ lymphocytes after *in vitro* short-term activation

The change of WASP-positive pattern in CD8+ lymphocytes was studied after *in vitro* short-term activation. CD8+ cells were purified in the following way. PBMNCs from normal individuals were incubated at 4°C with each 20 μL of CD4, CD56 and CD20 MicroBeads (Miltenyi Biotec) for 15 min, and cells were obtained after performing Vario MACS using an LD column and their purity was checked and used for the experiment. After *in vitro* short-term activation with ionomycin (25 ng/mL) and PMA (1 μg/mL) at 37°C for 4 h, CD8+ lymphocytes were performed FCM-WASP and analyzed by CellQuest software (Franklin Lakes, NJ, USA).

## Results

### Normal peripheral blood mononuclear cells showed two WASP-positive populations by FCM-WASP

We have detected two WASP-positive populations; $WASP^{low\text{-}bright}$ and $WASP^{high\text{-}bright}$, in normal PBMNCs using 3F3A5. In monocytes, these two distinct populations have never been detected, but only low-bright positive have been previously described. The pattern of these dual positive peaks showed some variation among individuals (Fig. 1). We first studied the pattern of the two WASP-positive populations in the different lymphocyte lineages including; CD4+, CD8+, CD20+, CD56+. The results showed that CD20+ cells were $WASP^{low\text{-}bright}$, whereas CD56+ cells were $WASP^{high\text{-}bright}$. In cases of CD4+ and CD8+ cell lineages, both $WASP^{low/high}$ positive peaks were observed. We subsequently studied the pattern of WASP in CD4+/CD45RA+ or CD45RO+ and CD8+/CD45RA+ or CD45RO+ lymphocytes. This demonstrated that CD45RO+ cells that were either CD4+ or CD8+ were $WASP^{high\text{-}bright}$, and that CD45RA+ cells with either CD4+ or CD8+ showed $WASP^{low\text{-}bright}$ (Fig. 2).

### Simultaneous staining with two anti-WASP antibodies revealed that the two WASP-positive peaks were detected with 3F3A5, but not with B-9 using

The two lymphocyte WASP-positive peaks observed using FCM-WASP were repeatedly detected using 3F3A5, but not with the B-9 antibody. To clarify these findings, we performed FCM-WASP on normal lymphocytes with simultaneous staining with 3F3A5 and B-9. The results clearly showed that the two WASP-positive peaks could be detected only with 3F3A5, but not with B-9 (Fig. 3A).

### No differences in the amount of WASP protein, or WASP mRNA levels were detected between $WASP^{low\text{-}bright}$ and $WASP^{high\text{-}bright}$ cell populations

We isolated the CD3+/CD45RA+ lymphocyte population as $WASP^{low\text{-}bright}$ cells, and CD3+/CD45RO+ population as $WASP^{high\text{-}bright}$ cells. We compared the amount of WASP protein and message levels between these two cell populations. We used WIP as a loading protein control and glyceraldehyde-3-phosphate dehydrogenase as a standard cDNA control. No obvious differences were observed at the WASP protein (Fig. 4A) or message levels (Fig. 4B) between the two populations.

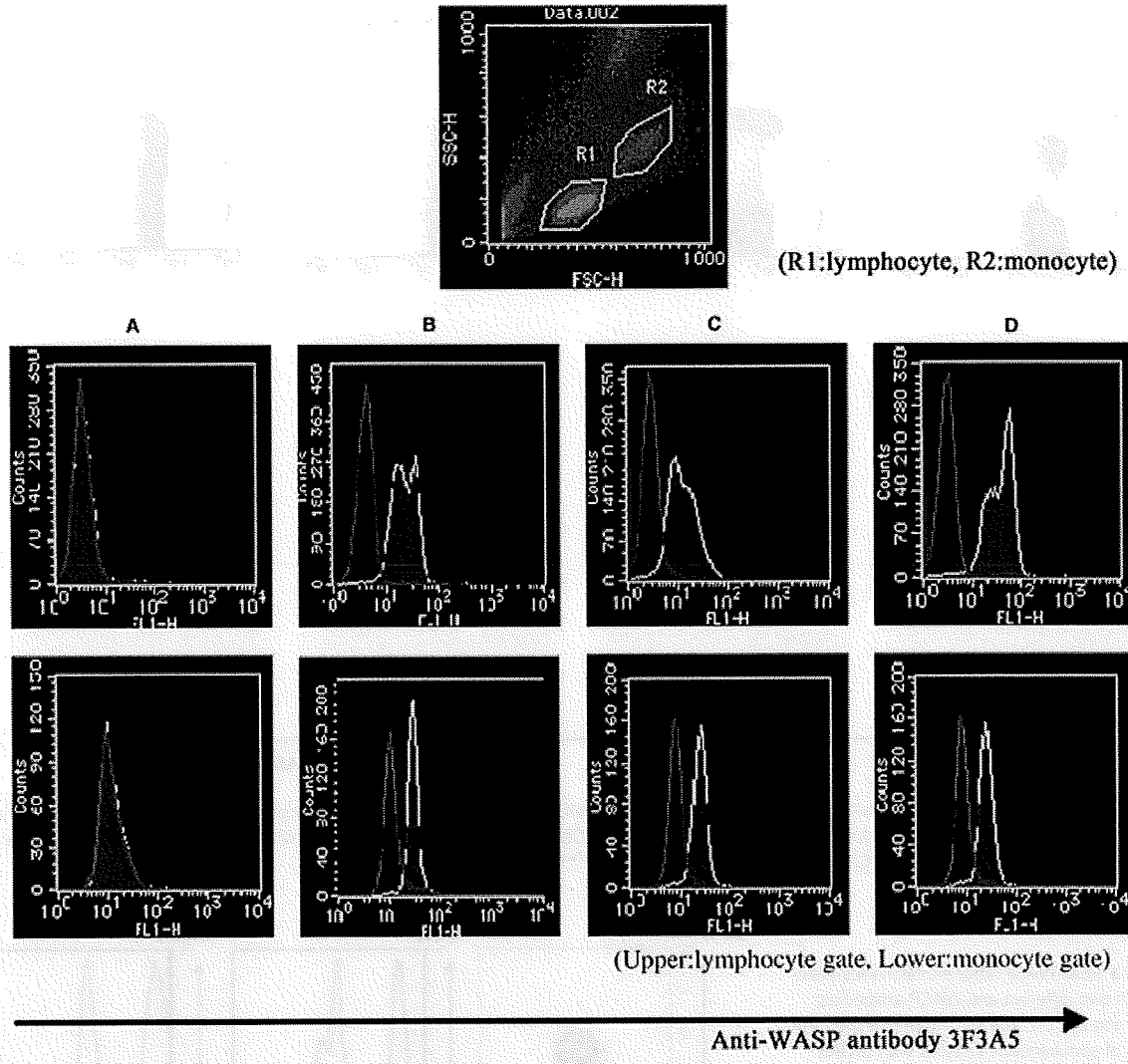


**Figure 1** Two WASP-positive populations were detected in lymphocytes by FCM-WASP. Using the anti-WASP antibody 3F3A5, a pattern of two WASP-positive populations; $WASP^{high\text{-}bright}$ cells and $WASP^{low\text{-}bright}$, were observed in lymphocytes from normal individuals. In contrast, monocytes from the same individuals showed only a single WASP-positive population. (A) a patient with WAS, (B–D) normal control individuals. The top figure shows analysis of the lymphocyte gate (R1), and the monocyte gate (R2). The middle 4 figures show the results of lymphocytes, the lower 4 figures show the results of monocytes.

### The WASP-positive pattern in CD8+ lymphocytes as seen by FCM-WASP changed during *in vitro* short-term activation

We next studied the effects of short-term lymphocyte activation on the WASP-positive cell pattern by FCM-WASP in the same lineage cells. We used CD8+ lymphocytes, because the CD8+ lineage has two populations most remarkably. To avoid synthesis of new WASP during activation, we settled on using a short-term (4 h) *in vitro* activation system and used 3F3A5 and B-9 antibodies together with FCM-WASP. We purified CD8+ lymphocytes by negative selection and these cells were used for FCM-WASP after PMA/ionomycin stimulation. After the short-term stimulation, the WASP-positive pattern showed significant up-regulation in FCM-WASP using 3F3A5, but not in FCM-WASP using B-9 (Fig. 5).

## Discussion

In our previous studies, we noticed that lymphocytes from healthy individuals showed two WASP expression

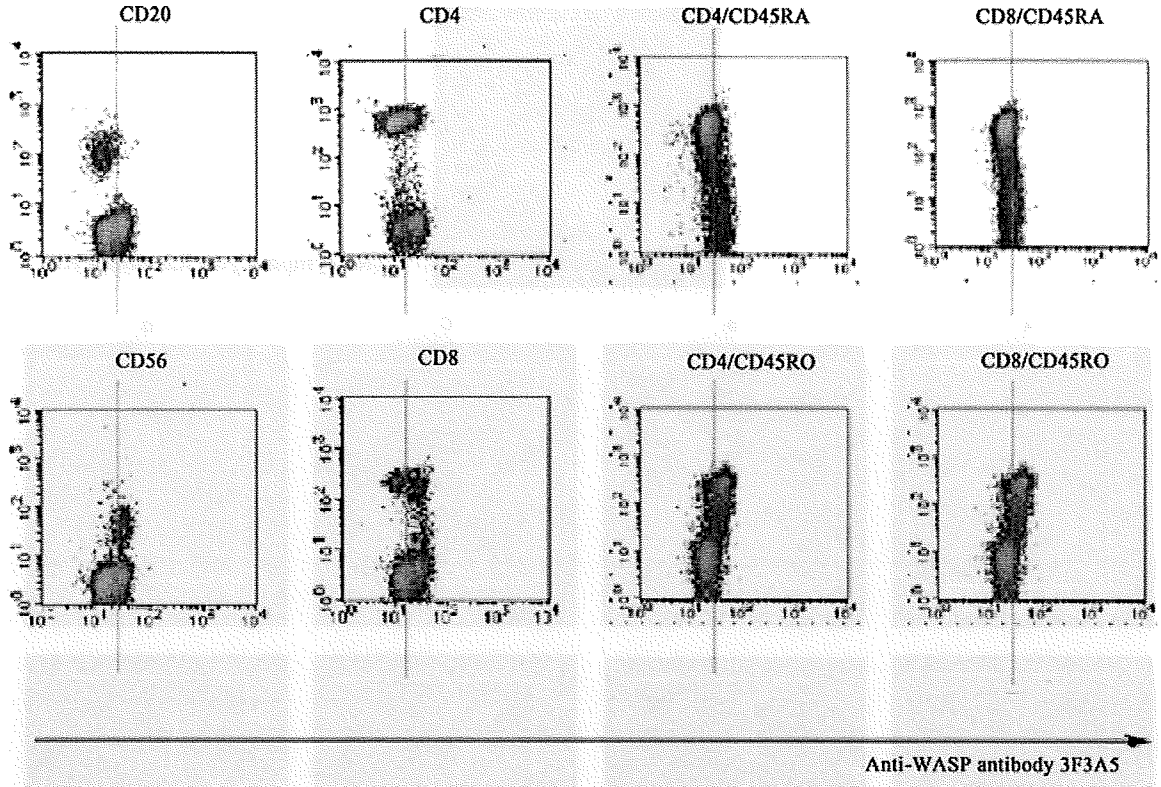


**Figure 2** Characterization of the constituent cell lineages of the each WASP-positive population. By dual/triple staining of intracellular WASP and surface cell markers, we determined that CD20+, CD4+/CD45RA+ and CD8+/CD45RA+ cells belonged to the $WASP^{low\text{-}bright}$ population, whereas CD56+, CD4+/CD45RO+ and CD8+/CD45RO+ cells belonged to $WASP^{high\text{-}bright}$.

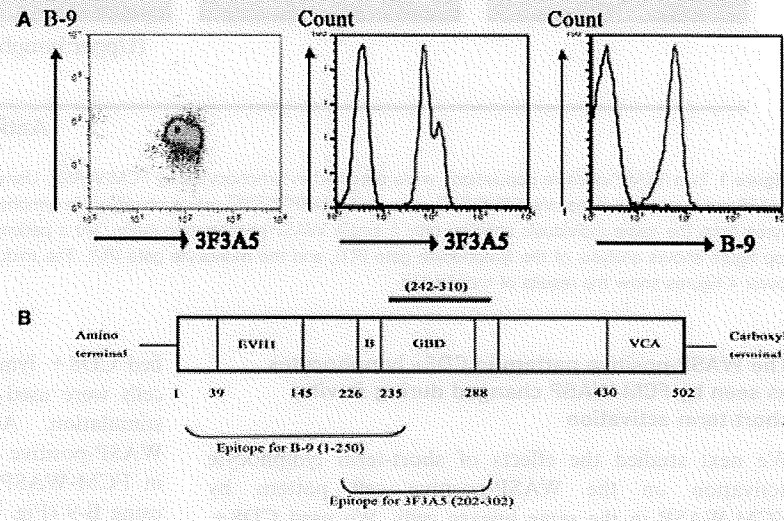


**Figure 3** FCM-WASP after simultaneous staining with two different anti-WASP antibodies; 3F3A5 and B-9 (A). The top figure indicates the results of simultaneous analysis with 3F3A5 and B-9, showing two distinct subpopulations using the 3F3A5 antibody, but a single positive population by B-9. The lower two figures show each independent result. The scheme showing the WASP structure (B) Figures indicate amino acid number. The underlined region (242–310) highlights a part of the GBD domain that is thought to be used for binding to the VCA domain in the inactive form of WASP. The scheme includes areas of possible epitopes for B-9 and 3F3A5 antibody binding represented. GBD domain (amino acids 235~288) is included within the 3F3A5 recognition site (amino acids 202–302).

profile populations; $WASP^{low\text{-}bright}$ and $WASP^{high\text{-}bright}$, using FCM-WASP. In this study, we confirmed two WASP-positive cell populations detected in the normal lymphocyte populations using FCM-WASP, and have proposed a possible mechanism causing the two populations.

We characterized the constituent cell lineage members of the each WASP-positive population. It was found that

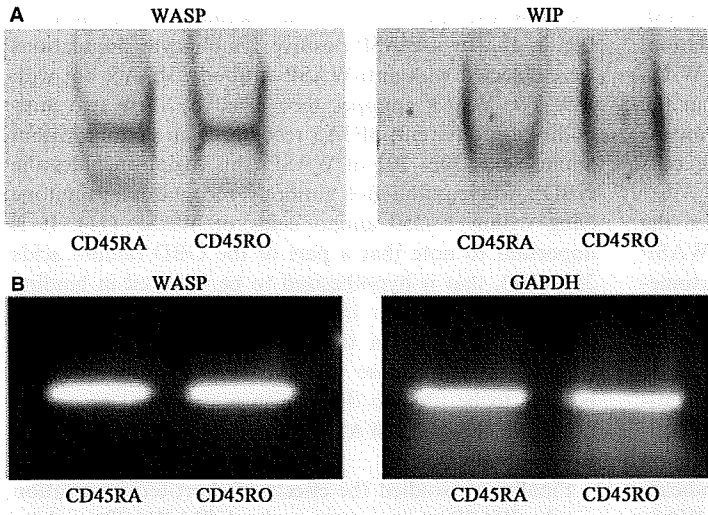


**Figure 4** Protein and message levels of WASP in CD3+CD45RA+ cells and CD3+CD45RO+ cells. No significant difference in WASP protein or message levels was observed between WASP$^{low\text{-}bright}$ (CD3+/CD45RA+) and WASP$^{high\text{-}bright}$ (CD3+/CD45RO+) populations. We used WIP as a loading protein control and glyceraldehyde-3-phosphate dehydrogenase (GAPDH) as a standard cDNA control. (A) Western blot analysis. (B) Reverse transcriptase (RT)-PCR analysis

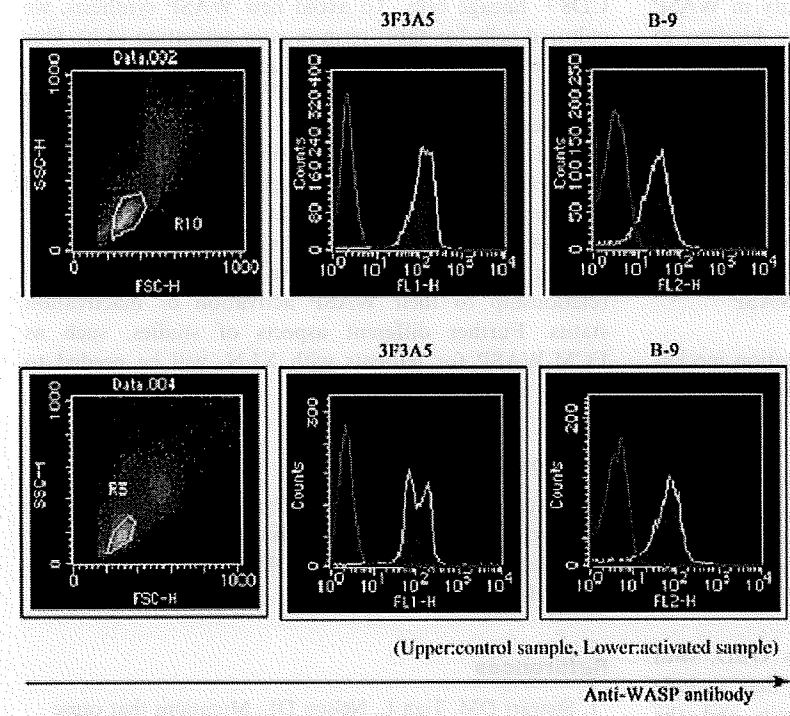


**Figure 5** Effects of short-term activation on the WASP expression pattern in CD8+ cells analyzed using FCM-WASP. Purified CD8+ cells were incubated with or without activation for 4 h and the WASP-expression patterns are compared by FCM-WASP. Using the 3F3A5 antibody, the pattern was clearly changed upon activation. In contrast, this postactivation pattern showed no change using B-9.

monocytes, CD20+ cells, CD4+/CD45RA+ cells and CD8+/CD45RA+ cells belonged to the WASP$^{low\text{-}bright}$ population, whereas CD56+ cells, CD4+/CD45RO+ cells and CD8+/CD45RO+ cells belonged to the WASP$^{high\text{-}bright}$ group. It is interesting that these results seem to be linked to the hierarchy of WASP dependency for cell proliferation/survival; which we have proposed based on various aspects of studies on WAS patients and their families. These studies included WAS carrier analysis (21, 22), mixed chimera analysis in WAS patients after hematopoietic stem cell transplantation (25) and cell lineage analysis in WAS patients who showed somatic mosaicism due to spontaneous reversion to normal from inherited mutations (26). Based on these results, we speculated that WASP-dependency was lower in monocytes and B cells compared to T cells, and among T cells, naïve T cells were less WASP dependent than memory T cells. Although we cannot accurately place the requirements for NK cells in this hierarchy for WASP dependency, recent reports suggested that NK cell WASP

dependency seemed high (27, 28). Thus, those less WASP dependent cells belong to the WASP $^{low\text{-}bright}$ population, while highly WASP dependent cells belong to the WASP$^{high\text{-}bright}$ population. This consistency suggests that the difference between the two WASP-positive populations is linked to the difference in the response of these cells through WASP-mediated stimulations.

Next, we studied the basis of differences between the two WASP-positive populations. Differences in WASP staining dot brightness as demonstrated by flow cytometry are generally considered as differences in the quantity of molecules detected by antibodies. Unexpectedly, however, we found that the two WASP-positive lymphocyte populations detected by FCM-WASP were only identified using the 3F3A5 antibody, but not with the B-9 antibody, which was confirmed by simultaneous staining with 3F3A5 and B-9 (Fig. 3A). These results indicate that the difference between WASP$^{low\text{-}bright}$ and WASP$^{high\text{-}bright}$ cells results not from any disparity in WASP expression, but from disparity in antibody binding to WASP that is likely dependant on protein confirmation. Accordingly, we purified CD3+/CD45RA+ and CD3+/CD45RO+ cells, representing WASP$^{low\text{-}bright}$ and WASP$^{high\text{-}bright}$ populations respectively, and performed Western blot and RT-PCR analysis. The results showed there was no apparent difference in WASP or *WASP* mRNA levels between them (Fig. 4A,B), supporting the speculation that there is no disparity in WASP expression between lymphocytes showing WASP$^{low\text{-}bright}$ and WASP$^{high\text{-}bright}$ staining patterns.

Recently, WASP autoinhibition and activation mechanisms have been reported (10). The crystal structure model of the WASP, indicated that it could exist in either an activated or an inactivated form based on intramolecular structural changes. WASP has an N-terminal Ena/VASP homology domain 1 (EVH1) domain, a Cdc42/Rac GTPase binding domain (GBD), a proline-rich domain, a G-actin binding verprolin homology (V) domain, a cofilin homology (C) domain and a C-terminal acidic (A) segment.

WASP interacts with Cdc42-GTP via its GBD, with multiple SH3 domain-containing proteins that include Nck via its proline-rich region, with actin and the ARP2/3 complex via its VCA domain. WASP is usually present in cells in a closed, inactive conformation due to intramolecular regulatory interactions that involve the C-terminal acidic domain and the basic region that precedes the GBD. Binding of Cdc42-GTP is thought to cause WASP conformational change, which allows the VCA domain to interact with and activate the Arp2/3 complex (10) (Fig. 3B).

Based on these auto-inactivation and activation mechanisms of WASP, we speculate that the results from the two WASP-positive lymphocyte populations detected by FCM-WASP are related to this mechanism. As shown in Fig. 4, the two WASP-positive lymphocyte populations were detected with anti-WASP antibody 3F3A5, not with B-9. The WASP epitopes recognized by these two antibodies are different; 3F3A5 recognizes an epitope within amino acids 202~302 of WASP (this region includes the GBD), whereas the B-9 antibody recognizes an epitope lying within 1~250 amino acids of WASP (11). It is important to note that a part of the GBD (amino acids 235~288), that is hypothesized to be involved in binding to the VCA domain in the inactive form of WASP, might be included in the 3F3A5 antibody recognition site. Thus, we propose that the 3F3A5 antibody might be able to be used to distinguish a structural or activation state change in WASP, that is not possible using the B-9 antibody.

Finally, we studied the effects of short-term activation on the WASP-positive pattern by FCM-WASP in these CD8+ lineage cells. To avoid new WASP synthesis, we cultured cells for short term *in vitro* activation (4 h). Our data revealed that short-term activation forced a dramatic change to the WASP$^{high\text{-}bright}$ pattern in the same cell lineage (Fig. 5).

Here we report a new possible application of flow cytometry for analysis of intracellular WAS protein and its structural and functional status. However, from our data we cannot determine the relation or possible function of the two WASP-positive populations and their relationship to their WASP activation or inactivation status. Further different aspects of studies, such as FCM-WASP for patients with XLN, will be needed to answer these questions.

## Acknowledgements

This study was supported by Grant-in-aid for Scientific Research from the Japanese Ministry of Health, Labor and Welfare (2542002917, 15COE011-02 and H19-Child-General-003).

## References

1. Stewart DM, Tian L, Nelson DL. Mutations that cause the Wiskott-Aldrich syndrome impair the interaction of Wiskott-Aldrich syndrome protein (WASP) with WASP interacting protein. *J Immunol* 1999;**162**:5019–24.
2. Derry JMJ, Ochs HD, Francke U. Isolation of a novel gene mutated in Wiskott-Aldrich syndrome. *Cell* 1994;**78**:635–44.
3. Symons M, Derry JMJ, Karlak B, Jiang S, Lemahieu V, Mccormick F, Francke U, Abo A. Wiskott-Aldrich syndrome protein, a novel effector for the GTPase CDC42Hs, is implicated in actin polymerization. *Cell* 1996;**84**:723–34.

4. Molina IJ, Sancho J, Terhorst C, Rosen FS, Remoid-O'Donnell E. T cells of patients with the Wiskott-Aldrich syndrome have a restricted defect in proliferative responses. *J Immunol* 1993;**151**:4383–90.
5. Cory GOC, MacCarthy-Morrogh L, Banin S, Gout I, Brickell PM, Levinsky RI, Kinnon C, Lovering RC. Evidence that the Wiskott-Aldrich syndrome protein may be involved in lymphoid cell signaling pathways. *J Immunol* 1996;**157**:3791–5.
6. Rudolph MG, Bayer P, Abo A, Kuhlmann J, Vetter IR, Wittinghofer A. The CDC42/Racinteractive binding region motif of the Wiskott-Aldrich syndrome protein (WASP) is necessary but not sufficient for tight binding to CDC42 and structure formation. *J Biol Chem* 1998;**273**:18067–76.
7. Higgs HN, Pollard TD. Regulation of actin filament network formation through arp2/3 complex: activation by a diverse array of proteins. *Annu Rev Biochem* 2001;**70**:649–76.
8. Gallego MD, Santamaria M, Pena J, Molina IJ. Defective actin reorganization and polymerization of Wiskott-Aldrich syndrome T cells in response to CD3-mediated stimulation. *Blood* 1997;**90**:3089–97.
9. Candotti F, Facchetti F, Blanzuoli L, Stewart DM, Nelson DL, Blaese RM. Retrovirus-mediated WASP gene transfer corrects defective actin polymerization in cell lines from Wiskott-Aldrich syndrome patients carrying null mutations. *Gene Ther* 1999;**6**:1170–4.
10. Kim AS, Kakalis LT, Abdul-Manan N, Liu GA, Rosen MK. Autoinhibition and activation mechanism of the Wiskott-Aldrich syndrome protein. *Nature* 2000;**404**:151–8.
11. Stewart DM, Treiber-Held S, Kurman CC, Facchetti F, Notarangelo LD, Nelson DL. Studies of the expression of the Wiskott-Aldrich syndrome protein. *J Clin Invest* 1996;**97**:2627–34.
12. Derry JMJ, Kerns JA, Weinberg KI, Ochs HD, Volpini V, Estivill X, Walker AP, Franke U. WASP gene mutations in Wiskott-Aldrich syndrome and X-linked thrombocytopenia. *Hum Mol Genet* 1995;**4**:1127–35.
13. Devriendt K, Kim AS, Mathijs G, *et al.* Constitutively activating mutation in WASP causes X-linked severe congenital neutropenia. *Nat Genet* 2001;**27**:313–7.
14. Aldrich RA, Steinber AG, Campbell DC. Pedigree demonstrating a sex-linked recessive condition characterized by draining ears, eczematoid dermatitis and bloody diarrhea. *Pediatrics.* 1954;**13**:133–9.
15. Sullivan KE, Mullen CA, Blaese RM, Winkeistein JA. A multi-institutional survey of the Wiskott-Aldrich syndrome. *J Pediatr* 1994;**125**:876–85.
16. Ochs HD. The Wiskott-Aldrich syndrome. *Semin Hematol* 1998;**35**:332–45.
17. Oda A, Ochs HD. Wiskott-Aldrich syndrome protein and platelets. *Immunol Rev* 2000;**178**:111–7.
18. Lutskiy MI, Rosen FS, Remold-O'Donnell E. Genotype-proteotype linkage in the Wiskott-Aldrich syndrome. *J Immunol* 2005;**175**:1329–36.
19. Folwaczny C, Ruelfs C, Walther J, König A, Emmerich B. Ulcerative colitis in a patient with Wiskott-Aldrich syndrome. *Endoscopy* 2005;**34**:840–1.
20. Johnston SL, Unsworth DJ, Dwight JF, Kennedy CTC. Wiskott-Aldrich syndrome, vasculitis and critical aortic dilatation. *Acta Paediatr* 2002;**90**:1346–8.
21. Yamada M, Ohtsu M, Kobayashi I, *et al.* Flow cytometric analysis of Wiskott-Aldrich syndrome (WAS) protein in lymphocytes from WAS patients and their familial carriers. *Blood* 1999;**93**:756–62.
22. Yamada M, Ariga T, Kawamura N, *et al.* Determination of carrier status for the Wiskott-Aldrich syndrome by flow cytometric analysis of Wiskott-Aldrich protein expression in peripheral blood mononuclear cells. *J Immunol* 2000;**165**:1119–22.
23. Ariga T, Yamada M, Wada T, Saitoh S, Sakiyama Y. Detection of lymphocytes and granulocytes expressing the mutant WASP message in carriers of Wiskott-Aldrich syndrome. *Br J Haematol* 1999;**104**:893–900.
24. Ariga T, Yamada M, Sakiyama Y. Mutation analysis of five Japanese families with Wiskott-Aldrich syndrome and determination of the family members'carrier status using three different methods. *Pediatr Res* 1997;**41**:535–40.
25. Yamaguchi K, Ariga T, Yamada M, *et al.* Mixed chimera status of 12 patient with Wiskott-Aldrich syndrome (WAS) after hematopoietic stem cell transplantation; evaluation by flow cytometric analysis of intracellular WAS protein expression. *Blood* 2002;**100**:1208–14.
26. Ariga T, Kondoh T, Yamaguchi K, Yamada M, Sasaki S, Nelson DL, Ikeda H, Kobayashi K, Moriuchi H, Sakiyama Y. Spontaneous in vivo reversion of an inherited mutation in the Wiskott-Aldrich syndrome. *J Immunol* 2001;**166**:5245–9.
27. Lutskiy MI, Beardsley DS, Rosen FS, Remold-O'Donnell E. Mosaicism of NK cells in a patient with Wiskott-Aldrich syndrome. *Blood* 2005;**106**:2815–7.
28. Orange JS, Ramesh N, Remold-O'Donnell E, Sasahara Y, Koopman L, Byrne M, Bonilla FA, Rosen FS, Geha RS, Strominger JL. Wiskott-Aldrich syndrome protein is required for NK cell cytotoxicity and colocalizes with actin to NK cell-activating immunologic synapses. *Proc Natl Acad Sci USA* 2002;**99**:11351–6.

STEM CELLS AND DEVELOPMENT
Volume 18, Number 8, 2009

DOI: 10.1089/scd.2008.0298

**ORIGINAL RESEARCH REPORT**

# Short-Term Culture of Umbilical Cord Blood–Derived CD34 Cells Enhances Engraftment Into NOD/SCID Mice Through Increased CXCR4 Expression

Norioki Ohno, Teruyuki Kajiume, Yasuhiko Sera, Takashi Sato, and Masao Kobayashi

Human umbilical cord blood (CB) has been used successfully in stem cell transplantation. A subpopulation of $CD34^+$ cells expresses chemokine receptor CXCR4 which is critical for bone marrow engraftment in human hematopoietic stem cells. Here, we demonstrate the effect of short-term culture on CXCR4 expression on umbilical CB-derived $CD34^+$ cells and subsequent engraftment capability in nonobese diabetic/severe combined immunodeficient (NOD/SCID) mice. Surface CXCR4 expression on $CD34^+$ cells increased after incubating the cells in medium alone for 2 h; this effect was blocked by the addition of AMD3100. No difference in CXCR4 mRNA expression was noted after incubating $CD34^+$ cells in culture for 2 h, although these cells showed significantly increased transmigrational activity toward SDF-1 and homing activity in NOD/SCID mice. Furthermore, cultured human $CD34^+$ cells showed improved engraftment into the bone marrow of NOD/SCID mice compared to noncultured or AMD3100-treated $CD34^+$ cells. These observations suggest that increased cell surface expression of CXCR4 on $CD34^+$ cells improved the engraftment of human umbilical CB cells into bone marrow through enhanced homing activity.

## Introduction

Human cord blood (CB), collected from the postpartum placenta and umbilical cord, is a rich source of hematopoietic stem cells (HSCs) and provides an attractive alternative to bone marrow or mobilized peripheral blood transplantation. However, a major disadvantage of CB transplantation is the relatively low number of HSCs in each CB unit that severely limits its usefulness in clinical transplantation [1]. Therefore, the development of ex vivo culture systems to expand CB HSC numbers is important to stem cell research and clinical application. Previous studies showed the transplantation of HSCs into nonobese diabetic/severe combined immunodeficient (NOD/SCID) mice to be a reliable model for the detection of regenerative human HSCs [2,3].

CXCR4 is the seven-transmembrane receptor of SDF-1 and is widely expressed in a variety of hematopoietic cell types, neuronal cells, and immature $CD34^+$ progenitor cells. The chemokine receptor, CXCR4, and its ligand, stromal cell-derived factor-1 (SDF-1, also known as CXCL12), play a central role in the migration, proliferation, differentiation, and survival of both murine and human hematopoietic stem/progenitor cells [4–7]. The SDF-1–CXCR4 axis has been proposed to be essential for the homing and repopulation of HSCs transplanted into immunodeficient NOD/SCID mice [8,9]. Recently, Kollet et al. [10] demonstrated that $CD34^+/CXCR4^-$ cells expressed intracellular CXCR4, the cell surface expression of which was stimulated by cytokines. The overexpression of CXCR4 on $CD34^+$ cells via gene transfer improved human stem cell motility, retention, and multilineage repopulation [11].

In the present study, we examined the effect of short-term culture on CXCR4 expression and engraftment in CB-derived $CD34^+$ cells transplanted into NOD/SCID mice. Our results demonstrated that short-term culture increased cell surface CXCR4 expression in $CD34^+$ cells and enhanced the retention of these human cells in mouse bone marrow through enhanced homing activity.

## Materials and Methods

### *Isolation of $CD34^+$ cells*

Umbilical CB was obtained from normal full-term deliveries, after first obtaining informed consent from all participants and the approval of the Chugoku-Shikoku Regional

Department of Pediatrics, Hiroshima University Graduate School of Biomedical Sciences, Hiroshima, Japan.